

AD-A104 604

NAVAL POSTGRADUATE SCHOOL MONTEREY CA
INVESTIGATION OF HEAT TRANSFER IN STRAIGHT AND CURVED RECTANGUL.—ETC(U)
JUN 81 R G HOLIHAN

F/6 20/13

UNCLASSIFIED

NL

Loc 1
ABOVE
100000



END
DATE ISSUED
10-81
OTIC

LEVEL

(2)

AD A104604

NAVAL POSTGRADUATE SCHOOL
Monterey, California



7/11/81
THESIS

INVESTIGATION OF HEAT TRANSFER IN STRAIGHT
AND CURVED RECTANGULAR DUCTS FOR LAMINAR
AND TRANSITION FLOWS

by

Robert George Holihan, Jr.

Jun 29 1981

12/91

Thesis Advisor

M. D. Kelleher

Approved for public release; distribution unlimited

FILE COPY

81928034

Unclassified

SECURITY CLASSIFICATION OF THIS PAGE (When Data Entered)

REPORT DOCUMENTATION PAGE		READ INSTRUCTIONS BEFORE COMPLETING FORM
1. REPORT NUMBER	2. GOVT ACCESSION NO.	3. RECIPIENT'S CATALOG NUMBER
4. TITLE (and Subtitle) Investigation of Heat Transfer in Straight and Curved Rectangular Ducts for Laminar and Transition Flows		5. TYPE OF REPORT & PERIOD COVERED Master's Thesis June 1981
7. AUTHOR(s) Robert George Holihan, Jr.	6. CONTRACT OR GRANT NUMBER(s)	
9. PERFORMING ORGANIZATION NAME AND ADDRESS Naval Postgraduate School Monterey, California 93940	10. PROGRAM ELEMENT, PROJECT, TASK AREA & WORK UNIT NUMBERS	
11. CONTROLLING OFFICE NAME AND ADDRESS Naval Postgraduate School Monterey, California	12. REPORT DATE June 1981	13. NUMBER OF PAGES 80
14. MONITORING AGENCY NAME & ADDRESS (if different from Controlling Office)	15. SECURITY CLASS. (of this report) Unclassified	
16. DECLASSIFICATION/DOWNGRADING SCHEDULE		
16. DISTRIBUTION STATEMENT (of this Report) Approved for public release; distribution unlimited		
17. DISTRIBUTION STATEMENT (of the abstract entered in Block 20, if different from Report)		
18. SUPPLEMENTARY NOTES		
19. KEY WORDS (Continue on reverse side if necessary and identify by block number) Taylor-Gortler Vortices, heat transfer, rectangular curved channel rectangular straight channel, Temsheet, laminar flows, transition flows		
20. ABSTRACT (Continue on reverse side if necessary and identify by block number) An experimental investigation was conducted to examine convection heat transfer in a duct of rectangular cross-section, having both a straight and curved flow passage. One wall was kept at a constant temperature, with the opposite wall being adiabatic. Heating of the air flowing in the channel was accomplished through Joulean heating of a wall composed of Temsheet. →		

Unclassified

SECURITY CLASSIFICATION OF THIS PAGE/When Data Envelope

Item #20 continued:

The experiments were conducted for steady state in Laminar and Transition flows. Development and propagation of the Taylor-Gortler vortices was shown to enhance the heat transfer rate in the curved section as compared to the straight section.

Accession For	_____
MSIS DATA	<input checked="" type="checkbox"/>
DTIC TAB	<input type="checkbox"/>
Unannounced	<input type="checkbox"/>
Justification	_____
By	_____
Distribution	_____
Availability	_____
Printed	_____
Dict	_____
A	

Approved for public release; distribution unlimited

Investigation of Heat Transfer in Straight and Curved
Rectangular Ducts for Laminar and Transition Flows

by

Robert George Holihan, Jr.
Lieutenant Commander, United States Navy
B.S., United States Naval Academy, 1968

Submitted in partial fulfillment of the
requirements for the degree of

MASTER OF SCIENCE IN MECHANICAL ENGINEERING

from the

NAVAL POSTGRADUATE SCHOOL
June 1981

Author: R. Holihan

Approved by: Mattie Kelleher Thesis Advisor

J. Gladby Second Reader

J. Marts Chairman, Department of Mechanical Engineering

William M. Tolles Dean of Science and Engineering

ABSTRACT

An experimental investigation was conducted to examine convection heat transfer in a duct of rectangular cross-section, having both a straight and curved flow passage. One wall was kept at a constant temperature, with the opposite wall being adiabatic. Heating of the air flowing in the channel was accomplished through Joulean heating of a wall composed of Temsheet.

The experiments were conducted for steady state in Laminar and Transition flows. Development and propagation of the Taylor-Gortler vortices was shown to enhance the heat transfer rate in the curved section as compared to the straight section.

TABLE OF CONTENTS

I.	INTRODUCTION -----	12
	A. TAYLOR-GORTLER VORTICES -----	12
	B. HISTORY -----	16
II.	INTENT OF THE STUDY -----	22
III.	EXPERIMENTAL WORK -----	24
	A. DESCRIPTION OF THE APPARATUS -----	24
	B. EXPERIMENTAL PROCEDURES -----	34
IV.	PRESENTATION OF DATA -----	41
	A. ANALYSIS -----	41
	B. RESULTS -----	45
V.	DISCUSSION AND CONCLUSIONS -----	51
VI.	RECOMMENDATIONS -----	63
	APPENDIX A: EXPERIMENTAL UNCERTAINTY -----	64
	APPENDIX B: SAMPLE CALCULATIONS -----	68
	A. SAMPLE CALCULATIONS DATA -----	69
	B. TEMPERATURE CALCULATIONS -----	70
	C. POWER CALCULATIONS -----	70
	D. AVERAGE HEAT TRANSFER COEFFICIENT (\bar{h}) -----	72
	E. AVERAGE NUSSELT NUMBER (\bar{Nu}) -----	72
	F. REYNOLDS NUMBER (Re) -----	72
	APPENDIX C: CORRELATIONS -----	73
	LIST OF REFERENCES -----	76
	INITIAL DISTRIBUTION LIST -----	80

LIST OF TABLES

TABLE I:	SUMMARY OF STRAIGHT TEST SECTION RESULTS -----	49
TABLE II:	SUMMARY OF CURVED TEST SECTION RESULTS -----	50
TABLE III:	CORRELATIONS -----	75

LIST OF FIGURES

Figure 1	Schematic of Taylor vortices between cylinders -----	13
Figure 2.	Schematic of Taylor-Gortler vortices between parallel plates -----	14
Figure 3.	Illustration of Equipment and Apparatus -----	25
Figure 4.	Cross-Sectional view of Channel -----	26
Figure 5.	Straight Test Section, detailed schematic --	29
Figure 6.	Curved Test Section, detailed schematic -----	30
Figure 7.	Thermocouple Placement in Test Sections -----	33
Figure 8.	Photograph of Test Channel -----	35
Figure 9.	Straight vs. curved section results for the present study -----	48
Figure 10.	Comparison of present data with Durao, Ballard and McCuen for Laminar Flows, Straight Section -----	55
Figure 11.	Comparison of present data with Durao and Ballard for Laminar Flow, Curved Section -----	56
Figure 12.	Comparison of present data for Transition Flows, Straight Section -----	61
Figure 13.	Comparison of present data for Transition Flows, Curved Section -----	62
Figure 14.	Energy balance in straight section -----	68

TABLE OF SYMBOLS

Symbol	Meaning	Units
Ac	cross sectional area of the channel	m^2
A_{PL}	area of the wall heater (Temsheet)	m^2
C_{pair}	specific heat of air at constant pressure	KJ/Kg $^{\circ}C$
d	height of the channel	m
De	Dean number	
D_h	hydraulic diameter	m
F_{wo-wi}	radiation shape factor	
\bar{h}	average heat transfer coefficient	$W/m^2 ^{\circ}C$
K_{air}	thermal conductivity of air	$W/m ^{\circ}C$
K_{INS}	thermal conductivity of insulation	$W/m ^{\circ}C$
\dot{m}	mass flow rate of air	Kg/sec
Nu	local Nusselt number	
\overline{Nu}	average Nusselt number	
\overline{Nu}_c	average Nusselt number in curved section	
\overline{Nu}_s	average Nusselt number in straight section	
Pr	Pradtl number	
P	atmospheric pressure	N/m^2
Q	rotameter flow percentage	
\dot{q}	volumetric flow rate of air	m^3/sec
Q_{air}	heat convected to the air	W
Q_{Li}	heat lost through inner wall (Plexiglass)	W
Q_{Lo}	heat lost through outer wall (Temsheet)	W
Q_p	power supplied	

Symbol	Meaning	Units
Q_r	heat transferred by radiation	W
Q_{wi}	heat transferred from the inner wall	W
Q_{wo}	heat transferred from the outer wall	W
R	gas constant for air	J/Kg °K
Re_d	Reynolds number based on channel height	
R_i	radius of curvature of inner wall	m
R_{PR}	electrical resistance of precision resistor	Ω
R_R	total radiation resistance	m^{-2}
Ta	Taylor number	
T_B	bulk temperature of the flow	°C
T_{EXIT}	flow exit temperature	°C
T_{IN}	average flow inlet temperature	°C
T_{INS}	temperature of the insulation	°C
T_{ROOM}	ambient temperature	°C
T_{OUT}	average flow outlet temperature after each test section	°C
T_{wi}	average temperature of inner wall	°K
T_{wo}	average temperature of outer wall	°K
V_{PR}	voltage across precision resistor	V
V_H	voltage across wall heater (Temsheet)	V
x^*	dimensionless axial length coordinate	
ϵ_{wi}	emissivity of inner wall (Plexiglas)	
ϵ_{wo}	emissivity of outer wall (Temsheet)	

Symbol	Meaning	Units
θ	temperature correction to standard conditions	
μ_{air}	dynamic viscosity of air	$\text{Kg}/\text{m}\cdot\text{sec}$
ρ	density of air	Kg/m^3
σ	Stefan - Boltzmann constant	$\text{W}/\text{m}^2\cdot\text{K}^4$
ΔT	mean temperature difference	$^{\circ}\text{C}$
ΔT_{INS}	temperature difference in insulation	$^{\circ}\text{C}$
ΔX_{INS}	thickness of insulation layers	m
ν_{air}	kinematic viscosity of air	m^2/s

ACKNOWLEDGEMENT

The author wishes to express his sincere appreciation and gratitude to Professor Matthew D. Kelleher for his invaluable assistance and direction in the formulation and development of this paper. Without his guidance this thesis would have been a near insurmountable effort.

Additionally, the shop personnel deserve a special thanks for their assistance and encouragement, and without whom the physical set-up of the experimentation could not have been accomplished.

This author must also pay a special thanks to his children, Keith and Robert, for their understanding in not having him home the many nights and weekends during the two years that this thesis culminates. And finally, to my wife, Susan, whose understanding, encouragement and love has been a source of inspiration and hope during this entire course of study. To her I must pay a very special thanks, she as truly has borne the burden of this academic endeavor and, without whom, this course of study and thesis could not have been accomplished.

I. INTRODUCTION

A. TAYLOR-GORTLER VORTICES

Since the early part of this century, considerable data and numerous studies have demonstrated that fully developed laminar flow along a concave wall does not remain two-dimensional [Refs. 1, 2, 3]. Instead, the flow forms a system of spiral vortices, of counter rotating pairs, whose axes are aligned in the direction of the principle fluid flow. This phenomenon, known as Taylor-Gortler vortices, is the result of the variations in the centrifugal forces acting on the fluid particles. Schematics of this type of motion are shown in Figures 1 and 2.

In a channel that is curved in the streamwise direction, the fluid particles near the center of the flow cross-section are subjected to higher centrifugal forces than those slower moving particles nearer to the boundary wall. Consequently, the tendency is for the fluid in or near the center of the channel to move outwardly towards the concave wall. This action then causes the fluid particles near the boundary wall to move in the spanwise direction, and finally move radially inward, replacing the outwardly moving particles. Once in the center of the channel these fluid particles come under those same stronger forces of the free stream velocity and continue the rotational effect. This cyclic motion causes the

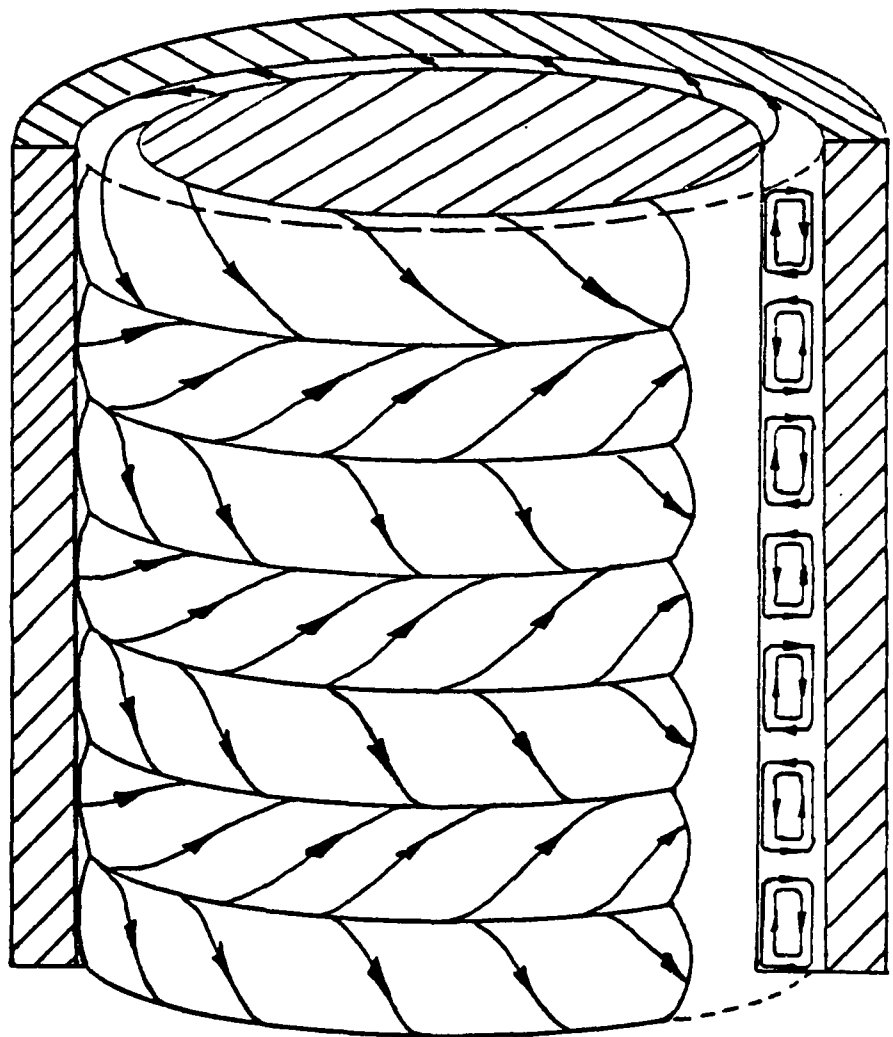


Figure 1. Schematic of Taylor vortices between cylinders

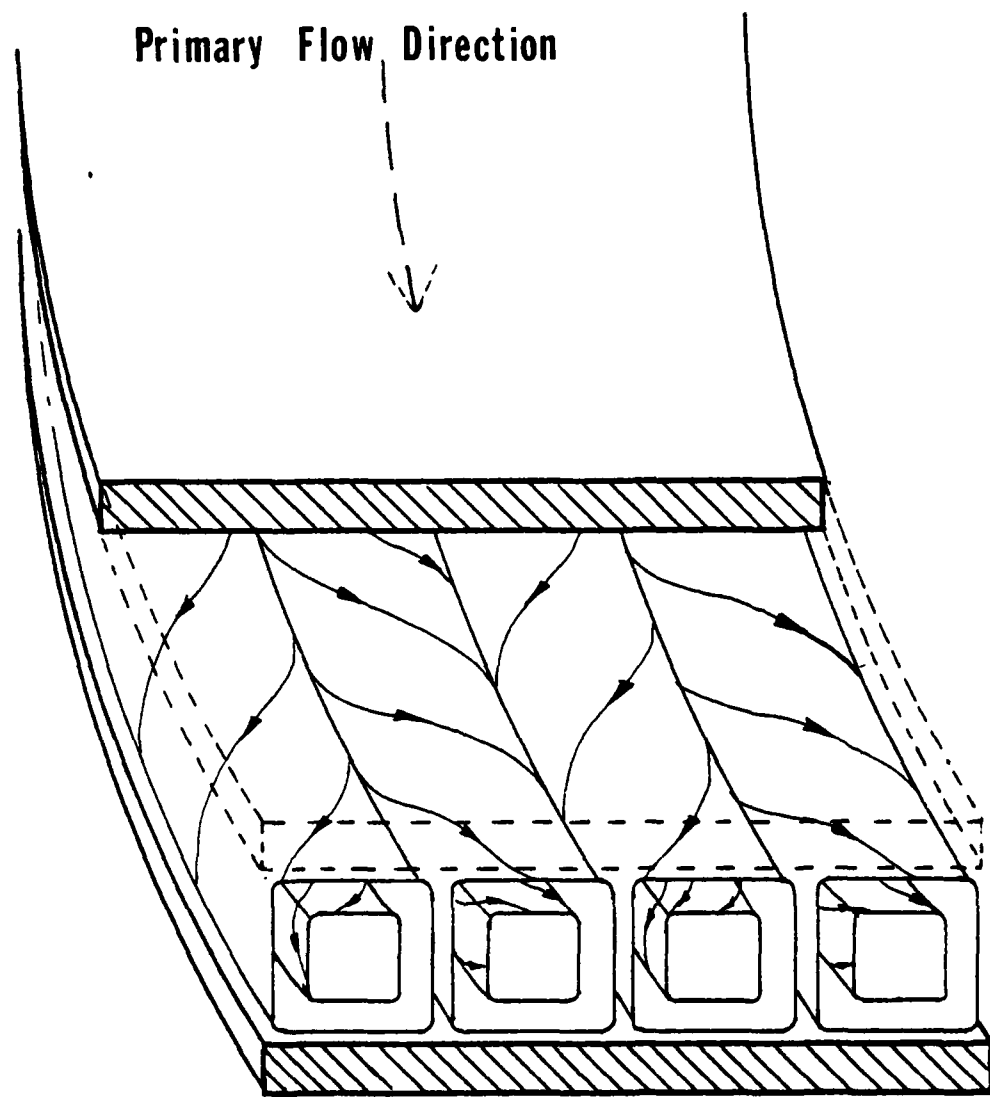


Figure 2. Schematic of Taylor-Görtler vortices between parallel plates

formation, and propagation, of the counter-rotating Taylor-Gortler vortices.

Although the Taylor-Gortler vortices are primarily a laminar flow phenomenon they may affect the transition from laminar to turbulent flows, and are therefore important to understand [Ref. 2]. The additional mixing provided by the secondary motion has been thought to account for the increase in the rate of heat transfer from concave curved walls versus straight walls [Ref. 4].

The Taylor-Gortler vortices appear to have similarities to other vortex flow patterns such as the longitudinal vortex rolls developed in the laminar forced convection heating of fluid layers between parallel plates [Ref. 5]. It has also been thought that the cross-hatching, observed in reentry vehicles, can be explained at least in part, by the presence of streamwise vortices [Ref. 6].

There are many possible applications that could result from a more thorough understanding of the Taylor-Gortler vortices and their effect on heat transfer and fluid flow characteristics. Applications, such as improved turbine blade cooling [Refs. 7, 8, 9], heat exchanger designs, as well as other such engineering designs and capabilities could take advantage of these vortices and improved heat transfer characteristics of the flow in the presence of these vortices.

B. HISTORY

The instability of an inviscid fluid rotating symmetrically about an axis, as in curved flow, was first considered by Lord Rayleigh in 1916 [Ref. 10]. In assuming that the fluid was non-viscous, he determined that a necessary condition, for the stability of an inviscid fluid motion, was that the circulation increased with increasing radius. G. I. Taylor, in 1923, [Refs. 1, 11] expanded the earlier works of Rayleigh by an extensive analytical and experimental study of viscous fluids. His investigations focused on the flow between two cylinders, in which the inner cylinder rotated while the outer cylinder remained stationary. Taylor ascertained that such couette flows became unstable when the value of the dimensionless Taylor number, defined as:

$$Ta = \frac{U_i d}{\nu} \sqrt{\frac{d}{R_i}} = Re \sqrt{\frac{d}{R_i}}$$

exceeded a critical value of 41.3. In the above equation, 'd' is the width of the gap, assumed small when compared to ' R_i ', the radius of the inner cylinder, ' U_i ' is the peripheral velocity of the inner cylinder, and 'Re' is the Reynolds number. Taylor determined that for those cases in which the value of the Taylor number became greater than the critical value, a secondary motion develops and the Taylor vortices form.

Instability of a similiar nature is also observed when a viscous fluid flows in a curved channel due to a pressure gradient acting along the channel wall. This problem was considered analytically first by W. R. Dean [Ref. 12] in 1928, for a channel formed by two concentric cylinders, where the radius of the inner cylinder was large in comparison to the small spacing between the inner and outer cylinder walls. Dean, in his studies, concluded that there would be an initiation of the flow instability, and the formation of vortices, (similiar to the Taylor vortices), when the Dean number, defined as:

$$De = Re \sqrt{\frac{d}{R_i}}$$

achieved a value greater than 36. In the above equation, the Reynolds number is based on the mean velocity of the unperturbed flow, 'd' represents the channel half-width, and 'R_i' is again the inner cylinder radius. The analytical work of Dean, was later verified by W. H. Reid [Ref. 13], using an approximate numerical solution.

H. Gortler [Ref. 2], in 1940, studied the stability of laminar boundary layer profiles, on curved walls under the influence of small disturbances. In his study, Gortler found that these disturbances were similiar in nature to those studied by G. I. Taylor, which had led to the fluid flow instability in the form of vortices. By approximate numerical

calculations, Gortler concluded that only on the concave boundary walls were the amplified disturbances produced, and that the overall flow profile appeared to remain laminar in nature. In 1955, Gortler's approximate results were verified, with an exact solution, by G. Hammerlin, as reported by H. Schlichting [Ref. 14] and then further substantiated in a more extensive numerical analysis by A. M. O. Smith [Ref. 3]. More recently, verification of these numerical solutions have been demonstrated by use of hot wire anemometry, laser doppler systems, and flow visualization techniques, [Refs. 15, 16], and in 1976, Y. Aihara [Ref. 17] conducted a non-linear analysis of the Gortler vortices.

With the growing interest in the effects of the secondary flows associated with the Taylor-Gortler vortices, numerous specific studies have been published concerning the influences of these vortices on the transfer of heat in both the laminar and turbulent flow regimes. F. Kreith [Ref. 4], in 1955, studied the influence of heat transfer with respect to the curvature of the boundary wall for fully turbulent flows, and concluded that the heat transfer from the heated concave boundary wall was considerably higher than that transferred from the convex boundary wall of the same curvature and under similiar turbulent flow conditions.

In 1965, L. Persen [Ref. 18], considering the special cases of very high and very low Prandtl number fluids, related the increase in heat transfer rate from a curved wall

to the presence of the Taylor-Gortler vortices. His conclusions were that the effect, of the development of the vortices, was to increase the rate of heat transfer through the boundary layer.

One of the first experimental works on the effects of the Taylor-Gortler vortices with respect to enhanced heat transfer was by P. McCormack, et al., [Ref. 19], published in 1970. With the data, they concluded that it was necessary to retain the non-linear terms of the flow equation in order that the complete theoretical solution of the effects of the Taylor-Gortler vortices on heat transfer be explained. In 1977, R. Kahawita and R. Meroney [Ref. 20], furthered McCormack's work and concluded that the higher order terms, as well as the normal velocity components of the main flow, became increasingly more significant to the calculations at smaller wave numbers.

In considering the forced convective heat transfer for fully turbulent flows, between horizontal parallel flat plates, Y. Mori and Y. Uchida [Ref. 5], in 1966, reported the formation of longitudinal vortex rolls with an axis parallel to the flow direction. These streamwise-axis directional rolls, similar to the Taylor-Gortler vortices, formed when a critical value of temperature difference between the plates was exceeded. In 1971, M. Akiyama, et al., [Ref. 21], confirmed the formation of these vortices at a critical

Rayleigh number of 1708, for the case of heating from the bottom plate surface.

There has been a rather limited amount of published literature regarding the flow and heat transfer in curved channels of rectangular cross-section. Much of the published literature involves the development of numerical approximations and solutions for heat and mass transfer in curved ducts of various geometries (most notably, that of circular and triangular ducts). K. Cheng and M. Akiyama [Ref. 22] developed a numerical solution for forced convection heat transfer with laminar flows in curved channels of rectangular cross-section, but only for small aspect ratios, (B/D ; where, 'B' is the channel width and 'D' is the depth of fluid flow). Using the fully elliptical forms of the transport equations, G. Yee and J. A. C. Humphrey [Ref. 23], developed a numerical solution for flows and boundary conditions similar to Cheng and Akiyama. K. Cheng, et al., [Ref. 24], in 1974, using numerical methods solved the Graetz problem for a curved channel of square cross-section ($B/D=1$).

In 1963, B. S. Petukhov and V. N. Popov [Ref. 25], obtained an analytical expression for the Nusselt number for the flow of an incompressible fluid with variable properties in a circular tube. In 1976, A. A. Shibani and M. N. Ozisik [Ref. 26] using matched asymptotic expansion techniques for

the case of uniform wall temperature, solved the heat transfer problem between parallel plates with turbulent flow, for a wide range of Prandtl numbers.

As to analytical and experimental studies of the parallel plate, channel flow heat transfer problem, Y. Mori, et al., [Ref. 27], obtained results for hydrodynamically fully developed flows with constant wall heat flux, in curved channels of square cross-section. W. M. Kays and E. Y. Leung, [Ref. 28], experimentally obtained solutions for turbulent flow heat transfer in a concentric circular tube annulus with fully developed velocity profile and constant heat rate per unit length, for a fluid of Prandtl number 0.7. M. Durao [Ref. 29] and J. Ballard [Ref. 30], reported results for large aspect ratio ($B/D = 40$) rectangular cross-sectional channels with laminar flows. P. F. Brinich and R. W. Graham [Ref. 31], reported results for turbulent flows in a rectangular curved channel with an aspect ratio of 6, for the inner wall heated, the outer wall heated, and both walls heated. In 1979, F. D. Haynes and G. D. Ashton [Ref. 32], in studying heat transfer from a river to its ice cover, reported results for rectangular cross-section channels of aspect ratio 10, and compared them to the data obtained by Ashton [Ref. 33], and Hsu [Ref. 34].

II. INTENT OF THE STUDY

The primary purpose of this study was to investigate the effect of the Taylor-Gortler vortices, on the enhancement of the heat transfer rate in a curved channel of rectangular cross-section and large aspect ratio. This investigation began with flow velocities that were in the laminar flow regime and continued into the transition region, between laminar and turbulent flow. Further, this study compared the heat transfer rate obtained in a curved section with the rate obtained in a straight section of identical aspect ratio.

It was expected that the presence of the Taylor-Gortler vortices would enhance the heat transfer process at all velocities in the flow regimes investigated. The cause of this would be the secondary flow velocity components of the vortices, transporting heated fluid from the concave boundary wall inward, while simultaneously displacing the cooler fluid particles in the center, causing them to move outwardly towards the heated concave wall.

This study was conducted using a single rectangular cross-sectional channel, that incorporated both a straight and a curved test section. The results obtained in the straight section were compared to those results obtained in the curved section, at the same flow velocities, in an effort to determine the effects of the Taylor-Gortler vortices on the

transfer of heat. Additionally, the results of both the straight and curved section tests were compared to the experimental results of Ballard [Ref. 30] and Durao [Ref. 29]. Those results of the straight section that fell into the laminar flow region, were also compared to the analytical solution as given by P. McCuen, et al., [Ref. 35]; while those in the transition region were compared to the experimental results of Kays and Lueng [Ref. 28], and the analytical results of the Dittus-Boelter equation [Ref. 38] and Eckert's equation [Ref. 39]. While these equations are for fully turbulent flows in circular tubes they have been used to compare turbulent flows in other geometry channels when the diameter of the tube is replaced by the hydraulic diameter (wetted perimeter divided by the cross-sectional area).

The straight section results, for transition flow, were also compared to the analytical solutions of Petukhov and Popov [Ref. 25] and Shibani and Ozisik [Ref. 26], the former for circular tubes while the latter is for parallel plates, both with fully turbulent flows.

The curved section results for flows in the transition region were compared to the experimental results of Brinich and Graham [Ref. 31], and also to the solutions of Petukhov and Popov, and of Shibani and Ozisik, mentioned above.

III. EXPERIMENTAL WORK

A. DESCRIPTION OF THE APPARATUS

A channel of rectangular cross-section built as described in references 29 and 30, was used to achieve the objectives of this study. The channel was manufactured from two 0.635 centimeter thick sheets of plexiglas, separated by 0.635 centimeter spacers whose inside lengths were used as the sides of the channel.

The channel, as shown in Figure 3, was composed of a straight section, 122.0 centimeters long, followed by a curved section of 180 degree arc. The interior concave wall of the curved section has a radius of curvature of 30.5 centimeters. The rectangular channel, with an aspect ratio of 40, was 0.635 centimeters high by 25.4 centimeters wide, with a cross-sectional area of 16.13 square centimeters and a wetted perimeter of 57.07 centimeters. A cross-sectional view of the channel, for both straight and curved sections, is shown in Figure 4.

The working fluid used in this investigation was air, at room temperature, which entered the channel via an entrance bell constructed of Plexiglas, which was connected to the straight section. The entrance bell was designed and manufactured in accordance with ASME nozzle standards, with an elliptical curved base on a major axis equal to ten inches

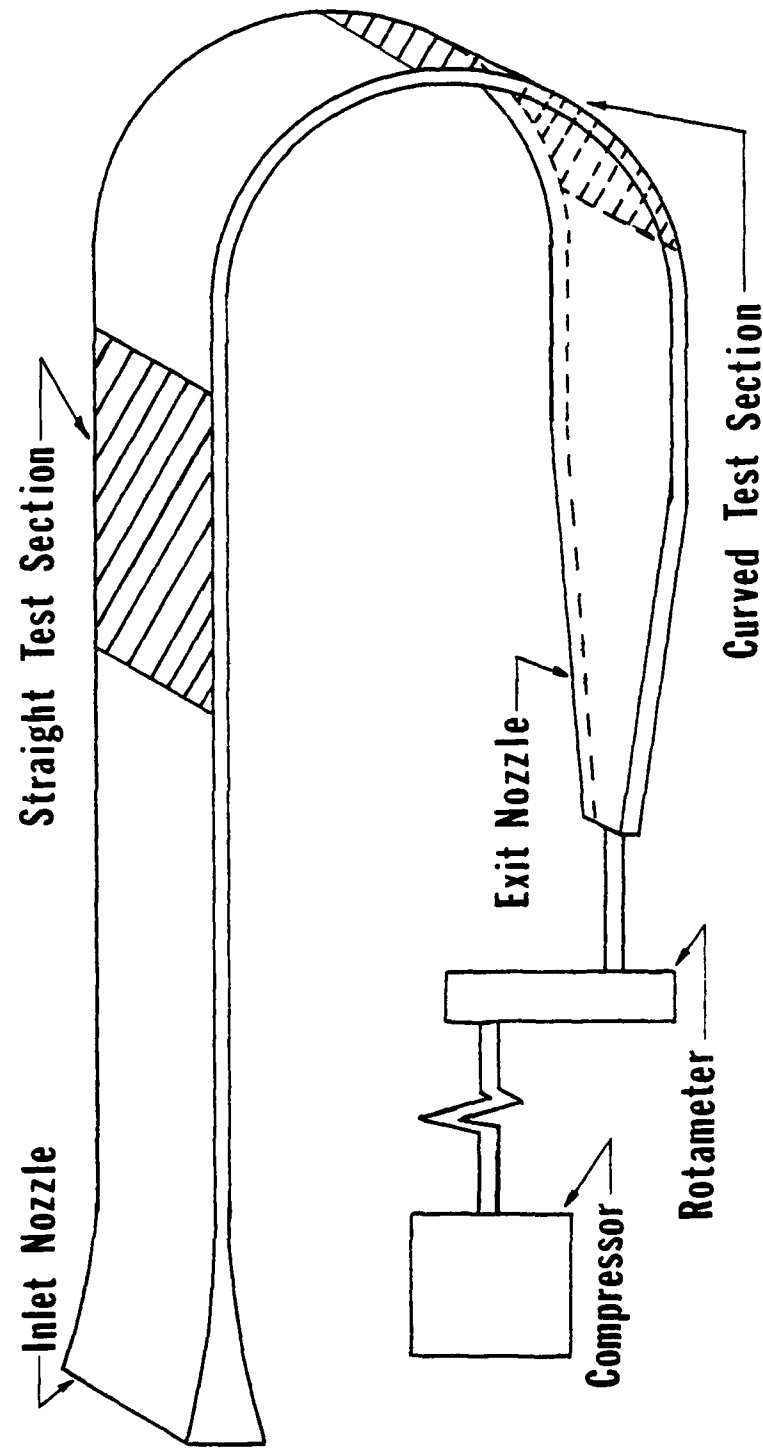


Figure 3. Illustration of Equipment and Apparatus

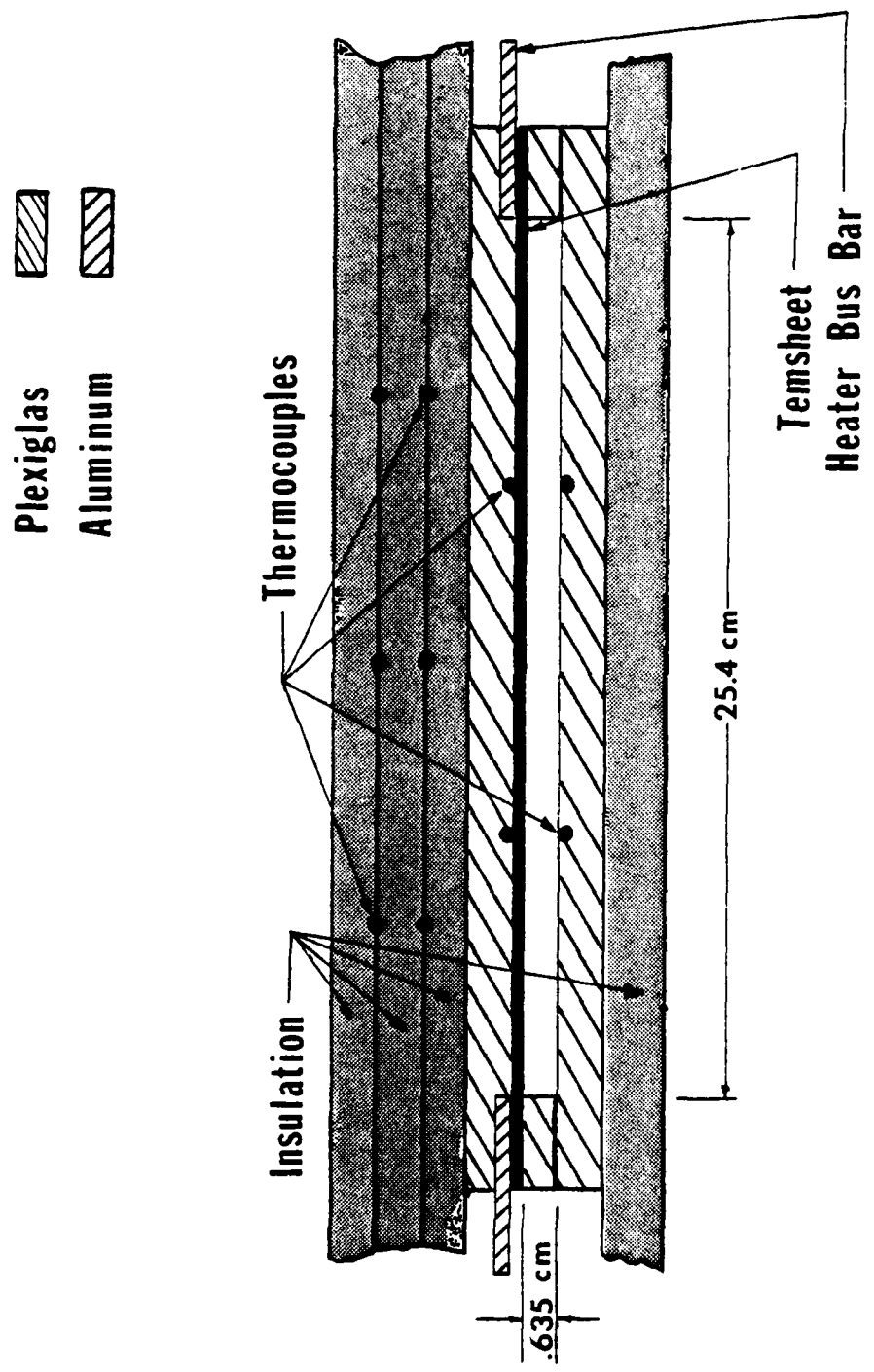


Figure 4. Cross-Sectional view of Channel

and a minor axis of one inch. In an attempt to prevent the introduction of dust and other foreign matter into the flow channel, cheese-cloth was attached to the opening of the entrance bell nozzle. After passing through the channel, the flow was directed through an aluminum exhaust nozzle which was connected, by 3/4 inch PVC piping, to a Fisher and Porter Company variable area flow meter model 10A3565A.

The rotameter, with a Bead Guide Tube number FP-1-35-G-10 and a 1GSVGT float serial number 68T60, at 100% full scale had a flow rate of 0.793 cubic meters of air per minute (28.0 standard cubic feet of air per minute at one atmosphere and 70°F).

The flow of air was drawn through the channel, piping and rotameter by a single electrically driven Spencer Turbo Compressor, 30 Hp. at 3500 rpm, rated at 550 cubic feet per minute at 70°F and one atmosphere. The flow rate was controlled by the use of valving both at the compressor and at the exit of the rotameter.

To obtain the experimental heat transfer data for this study, two test sections of the channel were constructed: (1) a straight test section, 29.2 centimeters in length, located far enough downstream to ensure hydrodynamically fully developed flow, with a heated test section area of 741.9 square centimeters. (2) a curved test section, 28.3 centimeters in length, subtending an arc of 53.1 degrees,

located in the lower half of the concave curved portion of the channel, with a test section area of 717.4 square centimeters.

In each of the test sections, the outer wall was modified as shown in Figures 5 and 6. Temsheet, a carbon impregnated porous paper with a property of uniform electrical resistivity, was glued to the interior surface of the outer wall of each of the two test sections. The flow of air was then to be heated by Joulean heating of the Temsheet. As the electrical resistance of Temsheet is not constant, but rather slowly variable with temperature, a precision resistor with an electrical resistance of 2.078 ohms was connected in series with the Temsheet to allow calculation of the instantaneous power being supplied.

The variables to be measured, in this investigation, were: (1) the inlet flow temperature for each of the test sections (T_{IN}), (2) the outlet flow temperature at the exit of each of the test sections (T_{OUT}), (3) the temperature of the heated boundary wall of each of the test sections (T_{wO}), (4) the temperature of the unheated boundary wall of each of the test sections (T_{wi}), (5) the flow temperature at the exit of the channel (T_{EXIT}), (6) the temperature between the two insulation layers for each of the two test sections (T_{INS}), (7) the voltage across the precision resistor (V_{PR}), (8) the heater voltage (V_H), and (9) the flow rate through the rotameter (Q).

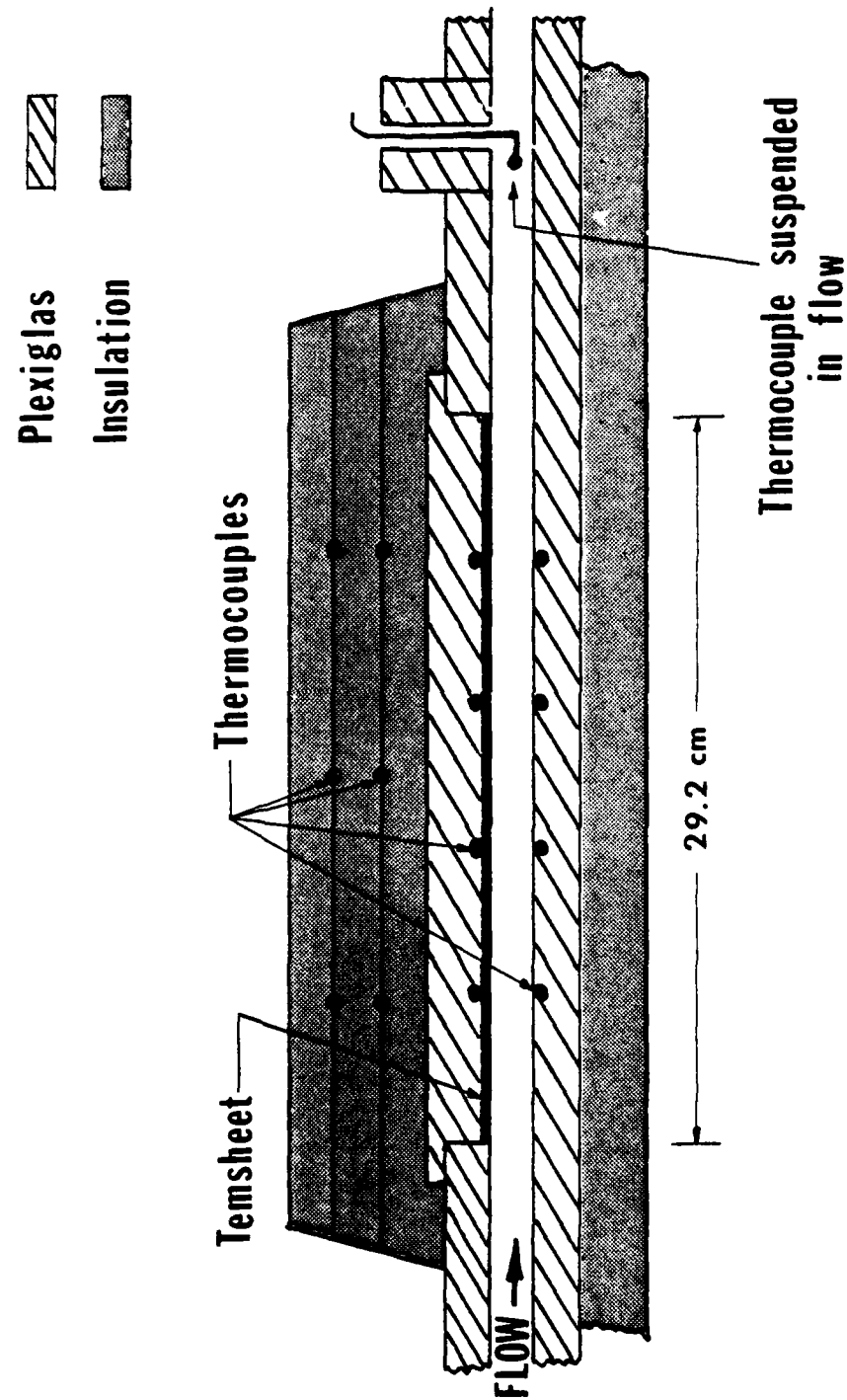


Figure 5. Straight Test Section, detailed schematic

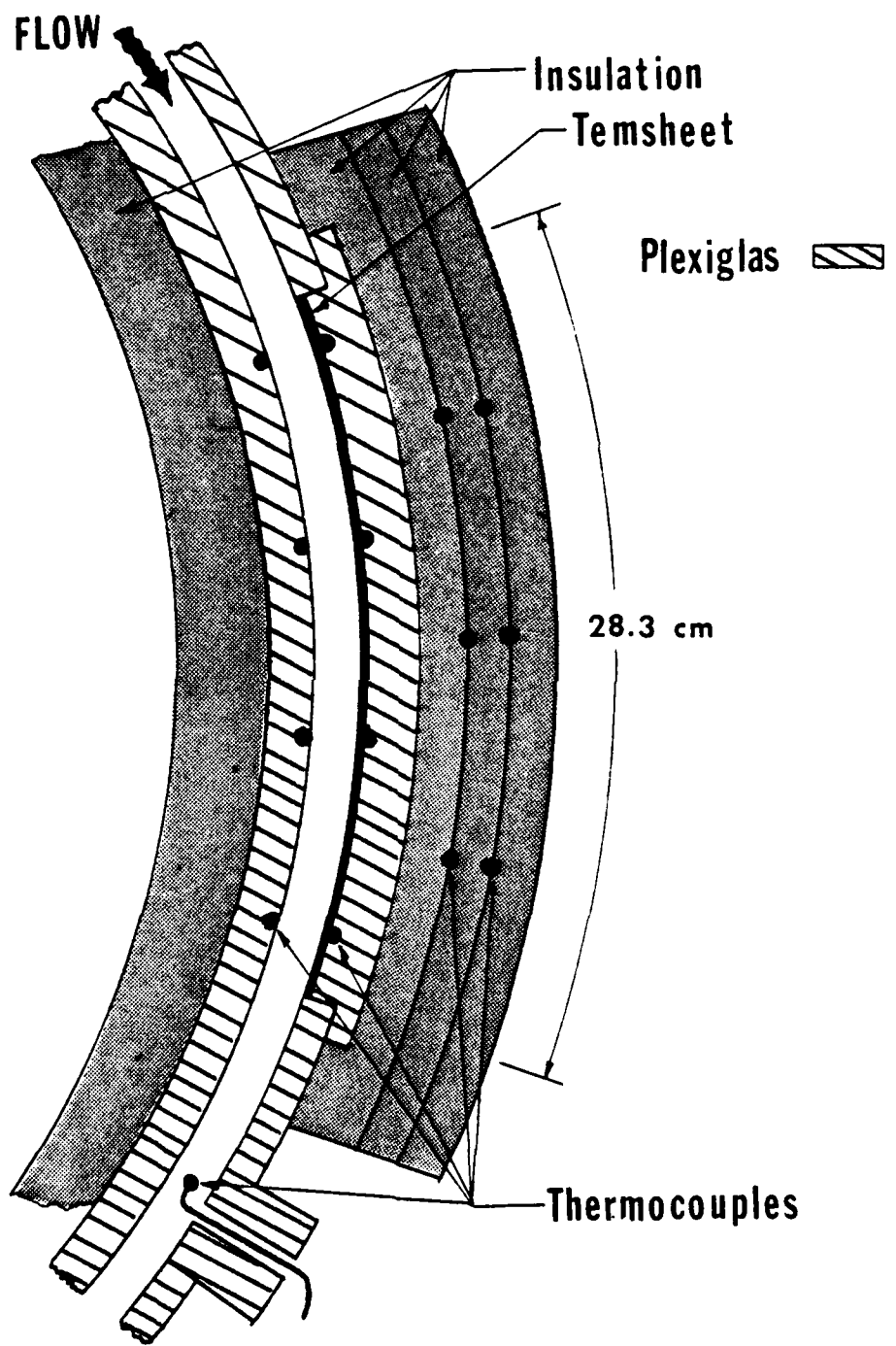


Figure 6. Curved Test Section, detailed schematic

The temperature measurements required above, as well as all other temperature measurements in this investigation, were made with Copper-Constantan thermocouples. All the thermocouples had been previously calibrated using a ROSEMOUNT Communtating Bridge model 920A, and a ROSEMOUNT Constant Temperature Bath model 913A, as outlined by Ballard [Ref. 30].

A total of sixty-four Copper-Constantan, glass insulated, 30 gauge thermocouples were constructed and inserted in specific locations to facilitate the measurement of the required temperatures. All the thermocouples were wired to a Hewlett Packard Data Acquisition System, model 2010c, which enabled an automatic printed record of the instantaneous reading for each thermocouple location. All the thermocouples were also connected to a Kaye Instrument Ice Point Reference, model K140-4, serial 1780.

In each of the test sections, five of the thermocouples were inserted between the first and second layers of ARMAFLEX 22 insulation, and another five inserted between the second and third layers. Each of these sets of five thermocouples were connected in parallel to facilitate the recording of an average value of the temperature (TINS) between the respective layers of insulation. Additionally, sets of four thermocouples, also connected in parallel to indicate average temperature, were inserted into the channel

at the following three locations: (1) the entrance of the channel, (2) the exit of the straight test section, and (3) the exit of the curved test section. At each of these three locations, the thermocouples were spaced five centimeters apart in the spanwise direction to allow reading of the bulk temperature of the flowing air.

In each of the two test sections, eight thermocouples were placed in direct contact with the Temsheet through small diameter holes drilled into the Plexiglas outer walls, with the thermocouple beads electrically insulated from the Temsheet with ENMAR Heat Resisting Glyceryl Phthalate. The final sixteen thermocouples were placed, eight to a test section in the Plexiglas unheated boundary wall, opposite those positioned in the Temsheet. A detailed sketch of the thermocouple placement is provided in Figure 7. The average heated outer wall temperature (T_{wo}), was provided by those thermocouples in contact with the Temsheet. The average unheated inner wall temperature (T_{wi}), was provided by the thermocouples embedded in the Plexiglas wall.

The thermal insulation consisted of layers of ARMSTRONG ARMAFLEX 22 Sheet Insulation, a flexible foamed plastic material, on the heated side of each test section, and black foam insulation one-half inches thick elsewhere. Three layers of the ARMAFLEX 22 insulation were used, each layer had a thickness of 0.636 centimeters, and covered an

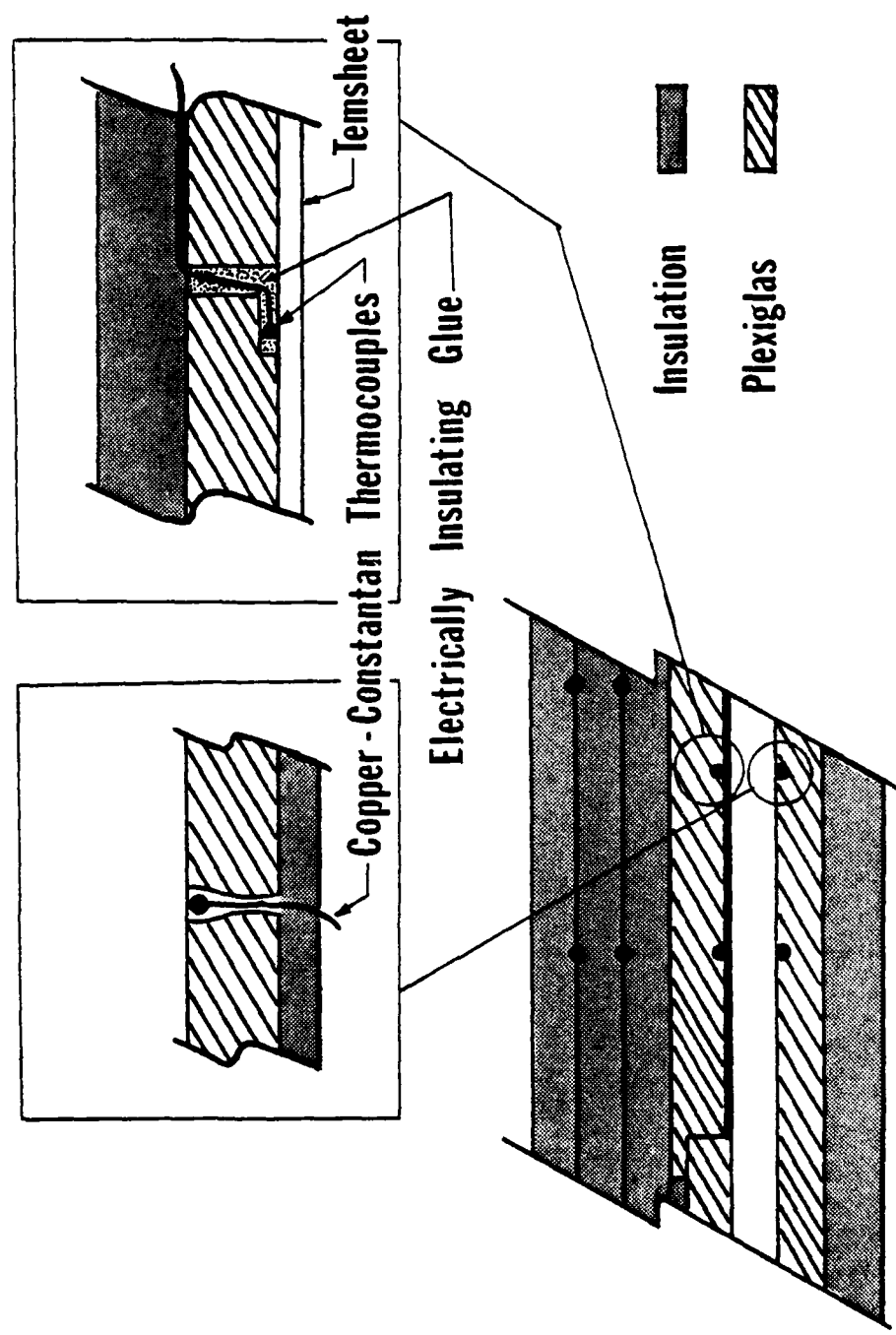


Figure 7. Thermocouple Placement in Test Sections

area slightly larger than the respective test section. These layers of insulation were used in the computation of heat flux losses to the environment, sample calculations of these losses are given in Appendix C. The rest of the channel was covered with the one-half inch thick Black foam insulation to reduce the losses to the surroundings through the plexiglas walls as the heated air transited the channel. The insulation was held in place by the use of Adhesive Heat Resistant ventilation Duct Tape as seen in Figure 8. The entire length of the channel as well as all the connections between the channel and the rotameter, were sealed with General Electric Silicone Rubber Sealant Caulk to ensure that there was no leakage of air into the channel or rotameter downstream of the entrance bell nozzle.

Two aluminum electrodes, 0.318 centimeters thick, were inserted in between the Temsheet and the plexiglas, in each of the test sections, as shown in Figure 4. The plates, with the Temsheet and aluminum electrodes were assembled in the channel with plastic teflon screws for the purpose of electrical insulation.

B. EXPERIMENTAL PROCEDURES

Experiments were conducted with the volumetric flow rate varied incrementally from 0.198 to 0.674 cubic meters

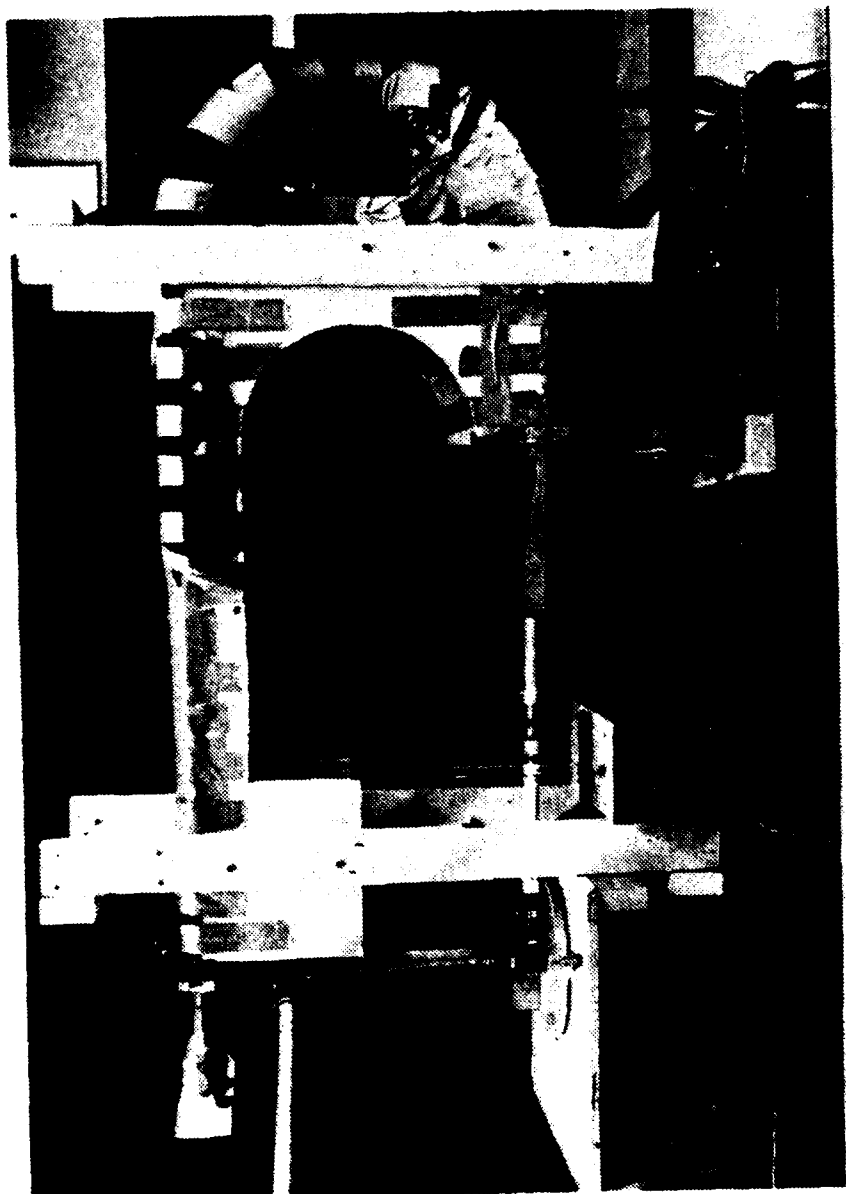


Figure 8. Photograph of Test Channel

of air per minute to correspond to particular Reynolds numbers. The data was recorded and calculations performed for each flow rate. The experimental procedures followed were the same for both the straight and curved test sections. The straight test section runs served as a baseline for the curved test section and allowed for comparison of the results. The appropriate electrical power required to heat the Temsheet boundary wall to approximately 50°C was determined through preliminary experiments. This temperature was chosen to allow at least a twenty degree celisus temperature difference between the unheated and heated boundary wall average temperatures and to facilitate achieving steady state conditions within a reasonable time span. Estimates of time to achieve steady state conditions and decisions as to data collection were also based on these preliminary test runs.

The determination as to what constituted a steady state condition required careful consideration in view of the multiple input variables and their effects on the results. The final criteria for steady state was based on three input variables: (1) flow rate percentage, as recorded from the rotameter; (2) heated boundary wall

temperature, as recorded from the thermocouples in that area; and (3) the heater voltage, as recorded on the voltmeter. When these conditions varied by less than two percent over a ten minute period, the experiment was considered to have achieved steady state. Under these conditions the assumption of steady flow and constant heat flux from the heated wall were assumed valid.

Originally, the time required to reach this steady state condition was found to be in the range of two hours, accordingly all runs were at two and one-half hours durations. Data was taken on one hour intervals for the first two hours and then at ten minute intervals for the next thirty minutes. Later it was found that the higher flow percentages for the curved test section, required about thirty minutes more time to full achieve steady state, so test runs with a flow percentage of sixty percent or greater were extended with three additional ten minute interval readings for a total time of three hours.

The instantaneous values for all the temperatures were automatically printed by the digital recorder in millivolts. A standard thermocouple table was used in conjunction with previously obtained thermocouple calibration data to convert the millivolts to degrees

Celsius. The volumetric flow rate was read directly from the installed rotameter as the percent of full scale flow. The instantaneous power supplied was calculated using the relationship:

$$Q_p = \frac{V_H}{R_{PR}} V_{PR}$$

Where the precision resistor voltage (V_{PR}) and the heater voltage (V_H) were recorded in volts from the installed voltmeter in the digital Data Acquisition System, and the electrical resistance of the precision resistor (R_{PR}) had been previously determined to be 2.078 ohms.

As the area of the curved test section was slightly less than the area of the straight test section, (0.0718 vs. 0.0742 square meters), the heat flux from the heated wall, of the respective test sections was different. The room temperature entering the test section was checked with the use of a mercury thermometer located in the vicinity of the apparatus.

During the preliminary test runs of the straight section, the thermocouple array recording the exiting temperature of the flow of air, was set at three millimeters from the heated wall. This was satisfactory at the lower volumetric flow rates, but at the higher flow rates it led to calculations in which the power

convected to the air was greater, by approximately fifteen to twenty percent, than the power being supplied to the heater. It was determined that the thermocouples were not indicating the correct bulk temperature of the exiting flow of air, but rather a higher value of temperature, this then resulted in an erroneously high value of convected heat transfer, and higher Nusselt numbers. To correct this, the system was allowed to run until the walls of the downstream curved section achieved steady state. Then, calculating the losses, by use of the thermocouples in between the insulation layers of the curved test section, and applying these losses to the entire curved section area, the energy loss was calculated. The flow exiting the channel was assumed to be thoroughly mixed and therefore the temperature as recorded by the positioned thermocouples, at the exit of the curved section, was used as an accurate representation of the average bulk exit temperature. With the final exit temperature and the losses now known, the temperature of the air as it exited the straight section was calculated.

To correct this condition, the thermocouples were inserted further in to the channel, or raised closer to the outer wall until the millivolt reading was compatible with the calculated correct temperature. After this procedure, accomplished at a flow rate of 0.595 cubic

centimeters of air per minute (75% of full scale) was completed, additional test runs were conducted at 0.555 and 0.635 cubic centimeters of air per minute (70% and 80% respectively), without adjusting the thermocouple positions, to check the accuracy. In each case, the temperature was within 0.25°C of what the energy balance indicated it should be.

It was later discovered that the curved section results had the same problem at flow rates greater than 0.595 cubic centimeters of air per minute. Since the channel construction is such that it does not allow further downstream data collection, and since the power difference was less than four percent it was decided to proceed with the correlation of the data and experimentation and note the discrepancies.

IV. PRESENTATION OF DATA

A. ANALYSIS

The uniform electrical resistivity of the Temsheet, approximated a constant heat flux surface for the heated wall. With insulation on the unheated wall the heat losses through that wall were negligible and the wall could be considered adiabatic. With the large aspect ratio of 40, the channel was considered to be approximately parallel plates. The straight portion of the channel upstream of the straight test section, was of sufficient length to ensure that the flow was hydrodynamically developed for the flow velocities investigated. Based on these assumptions, the experimental configuration was modeled as forced convection between parallel plates, for hydrodynamically developed and thermally developing flows, subjected to a constant heat flux. The boundary conditions are one wall at a constant specified heat flux, and the other wall insulated.

To analyze this condition, several quantities were defined as follows:

The average heat transfer coefficient between the heated wall and the flow of air was defined by the equation:

$$Q_{\text{air}} = \bar{h} A_{PL} \Delta T$$

where, ' Q_{air} ' was the heat convected to the air, ' h ' was the average heat transfer coefficient, ' A_{PL} ' was the area of the heated Temsheet for the section being tested, and ' ΔT ' was the difference between the average heated wall temperature (T_{wo}) and the average bulk temperature of the fluid (T_B). The average bulk temperature of the fluid was defined as the arithmetic mean of the fluid inlet bulk temperature (T_{IN}) and the fluid outlet bulk temperature (T_{OUT}). The delta temperature (ΔT) could then be expressed as:

$$\Delta T = T_{wo} - T_B = T_{wo} - \frac{T_{IN} + T_{OUT}}{2}$$

The actual heat convected to the air (Q_{air}) was calculated separately using the expression:

$$Q_{air} = \dot{m} c_{p,air} (T_{OUT} - T_{IN})$$

where ' $c_{p,air}$ ' was the specific heat of the air at constant pressure and ' \dot{m} ' was the mass flow rate of the air. The mass flow rate, is further defined as the product of the volumetric flow rate of the air and the local flow density of the air as it transits the rotameter. The volumetric flow rate of the air was corrected to standard conditions for the rotameter and the local flow density was calculated

assuming "perfect gas" behavior at constant pressure and utilizing the temperature of the air as it exited the channel (T_{EXIT}).

The average Nusselt number was then calculated from the average heat transfer coefficient, with the expression:

$$\overline{Nu} = \frac{h \cdot d}{K_{air}}$$

in which 'd' is the height of the channel and ' K_{air} ' is the thermal conductivity of the air evaluated at the average bulk temperature.

The Reynolds number was then calculated for each test run as follows:

$$Re_d = \frac{\dot{m} \cdot d}{\mu_{air} \cdot A_c}$$

where again ' \dot{m} ' and 'd' are the mass flow rate and height of the channel respectively, ' A_c ' is the cross-sectional area of the channel, and ' μ_{air} ' is the dynamic viscosity of the air evaluated at the exit flow temperature.

For the experiment runs utilizing the curved section, the Dean number, defined as:

$$De = Re_d \sqrt{\frac{d}{R_i}}$$

was also evaluated. In this equation, 'd' is again the height of the channel, and 'R_i' is the radius of curvature of the unheated wall surface of the channel (the convex wall).

The heat losses, by conduction, through the heated plate and the insulation, by conduction, were also calculated for each test section utilizing the expression:

$$Q_{lo} = \frac{\Delta T_{INS}}{(x_{INS}/K_{INS}) A_{PL}}$$

With ' ΔT_{INS} ' being the difference in temperature, as recorded, between the first and second layers of ARMAFLEX 22 insulation, and that recorded between the second and third layers. ' x_{INS} ' was the thickness of each layer of insulation, ' K_{INS} ' was the thermal conductivity of the insulation, and ' A_{PL} ' was again the area of the heated surface.

In order to verify that Q_{air} , as calculated by the temperature rise in the air, was actually the convection heat transfer from the Temsheet heated surface, an estimate of the radiation heat transfer was also calculated for each test run. The eight thermocouples in the lower Plexiglas surface measured the temperature of that surface and allowed the computation, utilizing the Stefan-Boltzman

law of radiation, of the radiated heat transfer (Q_r) with the expression:

$$Q_r = \frac{\sigma (T_{wo}^4 - T_{wi}^4)}{R_R}$$

where ' σ ' is the Stefan-Boltzman constant, and ' R_R ' is the total resistance to radiation heat transfer between the surfaces as computed by:

$$R_R = \frac{1}{A_{PL}} \left(\frac{1}{\epsilon_{wo}} + \frac{1}{\epsilon_{wi}} - 1 \right)$$

In the above equation, ' ϵ_{wo} ' is the emissivity of the heated Temsheet wall surface and ' ϵ_{wi} ' is the emissivity of the unheated adiabatic wall surface (Plexiglas).

A sketch of the control volume and the energy balance, with sample calculations for one test run, is given in Appendix B.

B. RESULTS

The data obtained from the experimental test runs were evaluated utilizing the expressions described in the previous section, and as illustrated in Appendix B. The results of the major variables are shown in tabular form, in Table I for the straight test section, and Table II for the curved test section. A plot of the average Nusselt

number versus Reynolds number, is given in Figure 9 for comparison of the two test sections. The uncertainty bands have been indicated for the plotted experimental data and a sample calculation for the complete error analysis is given in Appendix A.

As shown, the results indicate an increase in the rate of heat transfer with increasing Reynolds number for both the straight and curved test sections. Additionally, the heat transfer rate of the curved test section was higher than that of the straight test section for each Reynolds number investigated.

In investigating the results obtained, and considering those Reynolds numbers below 2000 (1025 based on this channel configuration) as laminar, at least squares straight line correlation of the data results in:

$$\overline{Nu} = 0.065 \quad Re_d^{0.67}$$

for laminar flows, and

$$\overline{Nu} = 0.117 \quad Re_d^{0.58}$$

for transition regime flows, in the curved test section.

With correlations of

$$\overline{Nu} = 0.983 \quad Re_d^{0.25}$$

for laminar flows, and

$$\frac{—}{Nu} = 0.110 \frac{0.56}{Re_d}$$

for the transition flows in the straight test section.

In the laminar flow regime, the increase in heat transfer was approximately fifteen percent, while in the higher transition flow region the increase was approximately thirty percent. This compares favorably to the earlier studies by Kreith [Ref. 4], in which he reported that the heat transfer rate along concave walls increased from twenty-five percent to sixty percent for Reynolds numbers, based on hydraulic diameter, between 10^4 and 10^6 , and Ballard [Ref. 30], who found an eleven percent increase in heat transfer rate for laminar flows.

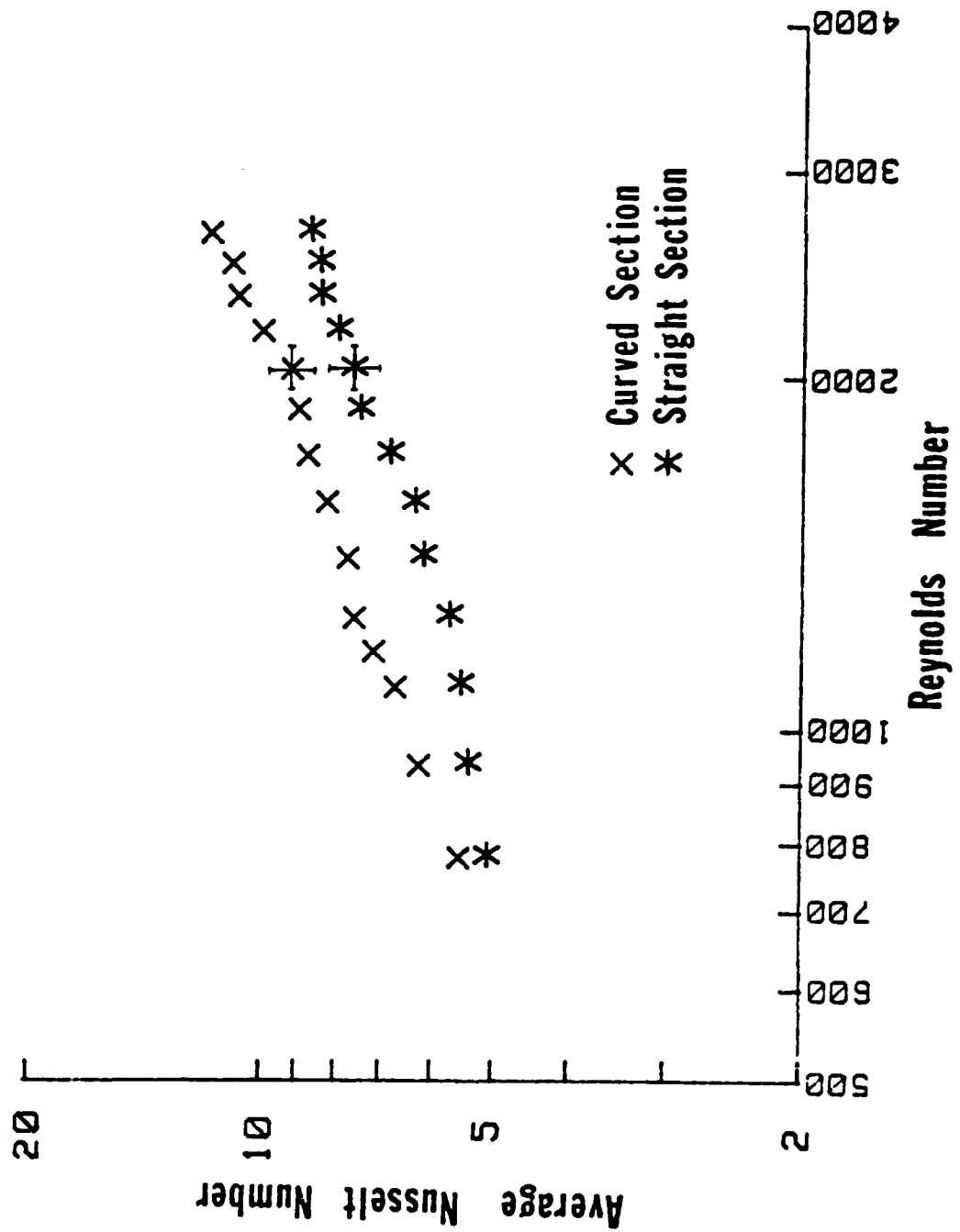


Figure 9. Straight vs. Curved Section results for the Present Study

TABLE I
SUMMARY OF STRAIGHT TEST SECTION RESULTS

Re_d	Q_{air} (W)	\bar{h} (W/m ² °C)	ΔT (°C)	\bar{Nu}
784	39.42	21.28	26.7	5.08
941	40.14	22.56	24.0	5.38
1099	43.26	23.11	25.2	5.51
1257	45.13	23.93	25.4	5.71
1414	51.80	25.89	27.0	6.18
1571	50.44	26.59	25.6	6.34
1729	53.50	28.61	25.2	6.83
1886	57.01	31.32	24.5	7.47
2042	59.24	31.99	25.0	7.63
2203	61.65	33.50	24.8	7.99
2361	62.97	35.30	24.0	8.42
2517	67.11	35.44	25.5	8.45
2675	69.14	36.39	25.6	8.68

TABLE II
SUMMARY OF CURVED TEST SECTION RESULTS

Re_d	De.	Q_{air} (W)	\bar{h} (W/m ² °C)	ΔT (°C)	\bar{Nu}
782	114	41.19	23.63	24.3	5.64
937	137	47.18	26.57	24.7	6.34
1092	159	50.88	28.56	24.8	6.81
1172	171	53.71	30.49	24.5	7.27
1251	183	57.16	32.32	24.6	7.71
1406	205	58.11	33.01	24.5	7.88
1570	229	62.63	35.12	24.9	8.38
1720	251	69.41	37.23	26.0	8.88
1883	275	70.90	38.29	25.8	9.13
2038	297	76.55	41.66	25.6	9.94
2196	320	80.36	42.72	26.2	10.19
2351	343	83.30	45.98	25.2	10.97
2505	366	88.82	46.87	26.4	11.18
2659	388	94.67	49.88	26.4	11.90

V. DISCUSSION AND CONCLUSIONS

With the measurement of the unheated wall and the air flow temperatures, it was indicated that there was a negligible difference between the fluid bulk temperature and the temperature of the unheated wall. Additionally, the energy balance and sample calculations, provided in Appendix B, demonstrate that the radiated heat transfer from the unheated wall surface is minimal. Thus it was assumed that the heat transfer to the flowing air was solely by convection from the heated Temsheet.

The high aspect ratio of the channel as discussed previously, provided the original basis for the assumption that the experimental apparatus, as configured, was one of infinite parallel plates. The experimental data, for those Reynolds numbers in the laminar flow region, tend to substantiate this assumption, in that they approach the theoretical limit for average Nusselt number of 5.385, for parallel plates with one wall heated at a constant heat flux and the opposite wall adiabatic [Ref. 37]. For a Reynolds number, based on hydraulic diameter, of 1835, the average value of Nusselt number obtained was 5.382.

With the formulation of the problem complete, the experimental data obtained can now be compared to the analytical solutions and experimental results of the same or similar

problem. That problem being, flow between infinite parallel plates with one wall at constant heat flux and the opposite wall adiabatic.

A comparison of the experimental results obtained in this study and the experimental results of Durao [Ref. 29] and Ballard [Ref. 30] (who investigated the problem solely for laminar flows), are shown in Figure 10, for the straight section, and Figure 11, for the curved section. In both these studies, as in this investigation, the channel has an aspect ratio of 40, and the experimental procedures were similar. It can be seen that the results obtained in this study, in the laminar flow regime, appear to be in agreement with the data obtained previously for both test sections. Additionally, numerical correlations of the present data, as given earlier, for the laminar flows compares favorably to the numerical correlations of both Durao and Ballard, for Reynolds numbers greater than 600, as given in Appendix C. In the two investigations, mentioned above, comparisons were made to the analytical studies of McCuen, et. al. [Ref. 35], for heat transfer between infinite parallel planes with constant wall temperatures and heat flux. Ballard also compared his data to the Wosse-Schimdt solution [Ref. 36], for heat transfer in tubes and annular passages. In both the Durao and Ballard studies, the experimental data compared relatively well to the predicted solutions of McCuen, et al. A curve of the predicted solution

of the McCuen, et. al. study is shown in Figure 10. The restrictions of that study were as follows:

1. the velocity profile is fully established.
2. the fluid transport properties and density are assumed constant.
3. axial heat conduction is negligible.
4. viscous energy dissipated is negligible.
5. conditions are invariant with time (steady state).

All these restrictions have been accounted for in the design of the experimental configuration and/or verified in the experimental processes. A dimensionless axial length coordinate defined as:

$$x^* = \frac{x}{D_h \text{Re} \text{Pr}}$$

was calculated for 'x' equal to 29.2 centimeters (the length of the straight test section). In this equation, 'Pr' is the Prandtl number of air, taken as 0.7, 'D_h' is the hydraulic diameter (1.239 centimeters), and 'Re' is the Reynolds number, based on the hydraulic diameter.

Based on the values of x*, it was determined that the experiments, for laminar flows, were in the thermal entrance region. It was therefore decided to integrate the expression of the local Nusselt number as given by McCuen, et. al. [Ref. 35]:

$$\text{Nu} = \frac{1}{0.67095 x^{*(1/3)} - 2(1 + \frac{Q_{wi}}{Q_{wo}})x^*}$$

for the small values of x , in order to obtain the following expression for the average Nusselt number:

$$\overline{Nu} = - \frac{3}{4(1 + \frac{Q_{wi}}{Q_{wo}})x^*} \ln \left(1 - \frac{2}{0.67095} \left(1 + \frac{Q_{wi}}{Q_{wo}} \right) x^{*- (2/3)} \right)$$

In this expression, Q_{wi} was the heat convected to the fluid from the unheated wall, and Q_{wo} was the heat convected to the fluid from the heated wall. In accordance with the previous assumptions, Q_{wi} was considered equal to zero, and Q_{wo} was considered equal to Q_{air} , and the average Nusselt number could then be calculated, and the expression reduces to:

$$\overline{Nu} = \frac{-0.75}{x^*} \ln \left(1 - \frac{2}{0.67095} x^{*- (2/3)} \right)$$

This value of average Nusselt number was plotted for values corresponding to an x^* less than 0.042, as this represents the maximum value for which the analytic solution for Nusselt number is valid. This value of x^* , (0.042), for x equal to 29.2 centimeters, equates to a Reynolds number value of approximately 800, based on hydraulic diameter (or 411 based on the channel height).

The graphical representation shows that the experimental results of this study as well as those of Ballard and Durao plotted above the analytical solution. This difference can probably be explained, at least in part, by the difference in geometries used in the studies, and by the limitations inherent in any experimental work. The side wall effects and the inability to totally account for all the heat transfer processes

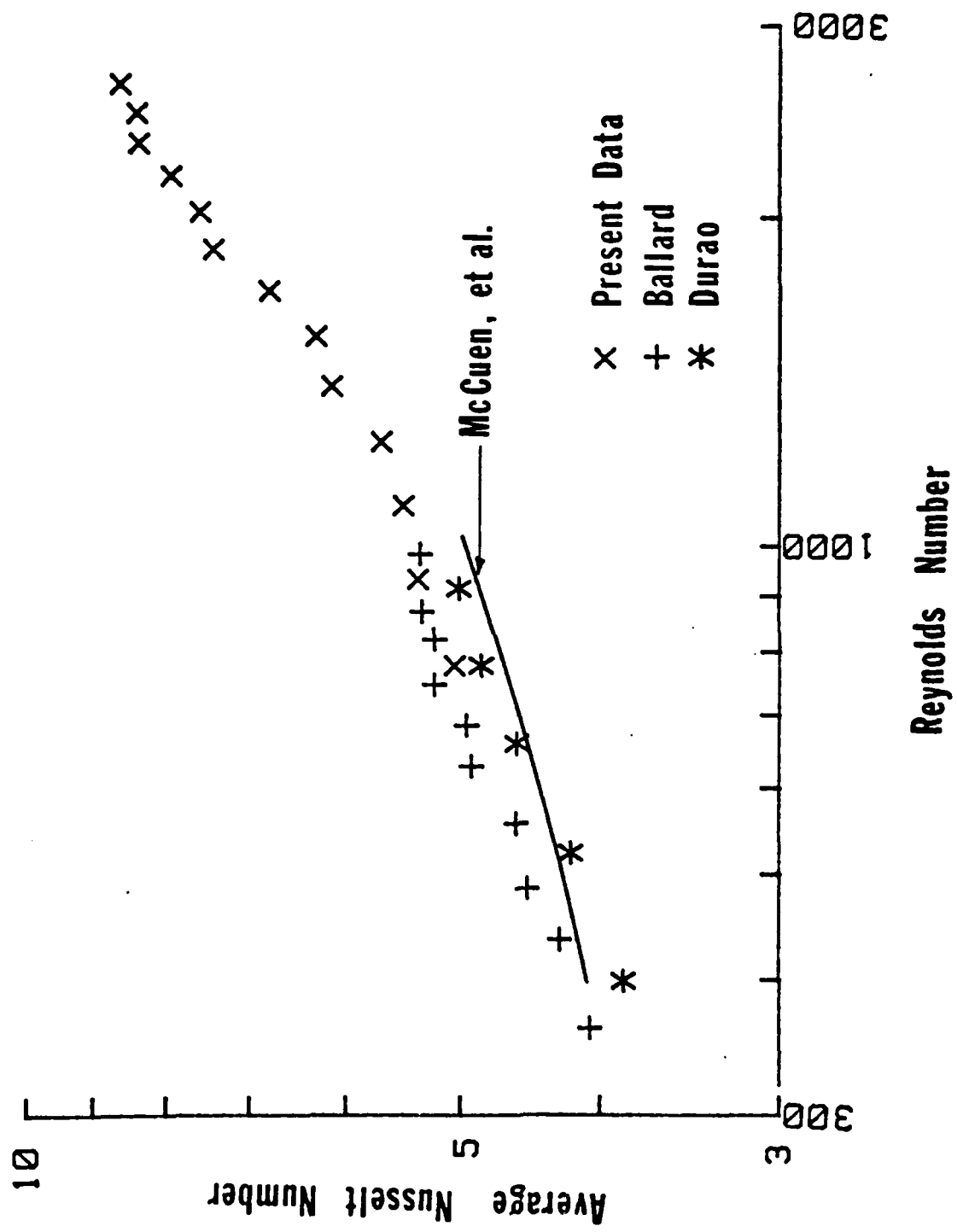


Figure 10. Comparison of present data with Durao, Ballard and McCuen for Laminar Flows, Straight Section

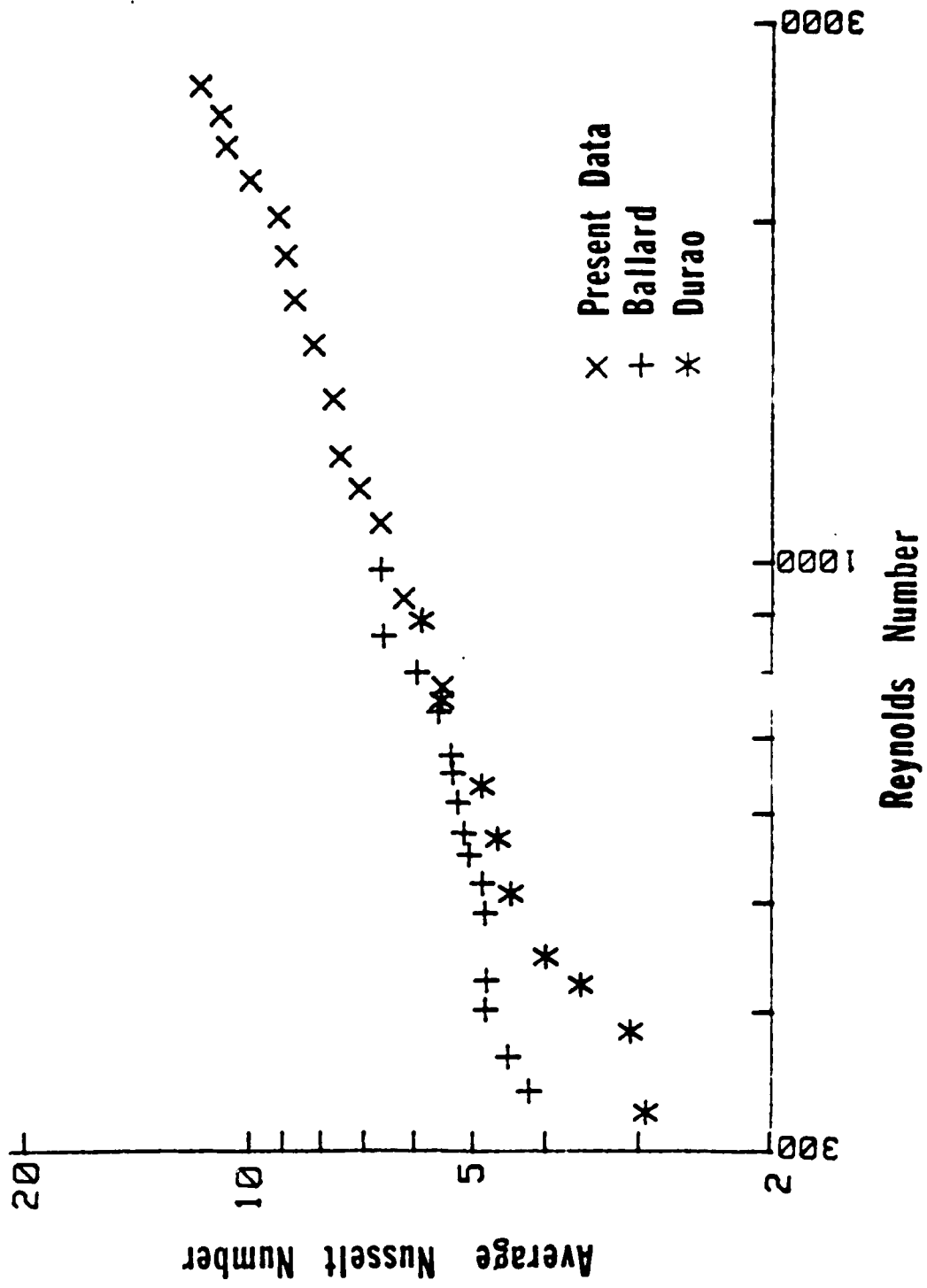


Figure 11. Comparison of present data with Durao and Ballard for Laminar Flow, Curved Section

and/or losses could account for the differences of approximately nine to ten percent.

In the comparison of the experimental results obtained in this study for those flows not in the laminar regime, the comparison and correlation was made to those analytical solutions and experimental results for completely turbulent flows. For the most part, the analytical solutions are valid for Reynolds number values greater than 10^4 (equating to a Reynolds number of 5128 in this study), and tube flow (or other geometries based on hydraulic diameter).

A graphical comparison of the results obtained in the straight test section runs with the analytical solutions and other experimental results is made in Figure 12. The plot shows the curve of heat transfer in a straight tube for constant wall temperature, as given by the Dittus-Boelter equations [Ref. 38]:

$$Nu = 0.023 Re^{0.8} Pr^{0.4}$$

and by the empirical relation as given by E.R.G Eckert [Ref. 39]:

$$Nu = \frac{0.0396 Re^{0.75} Pr}{(1 - \frac{44}{Re^{0.125}})}$$

This analytical expressions when extrapolated down show some agreement with the values obtained at flow rates between forty and seventy percent of the rotameter full scale. Unfortunately, those values obtained at the higher flow rates showed less of a correlation than those mentioned above. These results,

obtained for volumetric flow rates higher than seventy percent may have been affected by the fact that they were near the top end of the rotameter scale, and therefore, may inherently be somewhat less accurate than the mid-scale readings. The thermocouple problem discussed previously, may also have contributed to the decrease in correlation.

When extrapolated down, the experimental results of Kays and Leung [Ref. 28], for heat transfer in annular passages, with one wall heated at a constant heat rate, and r^* equal to 1.0, (where r^* is the annulus radius ratio r_i/r_o), equivalent to parallel plates, appears to correlate well with the present results. This extrapolation, was again utilizing a least squares straight line correlation, as given in Appendix C. Also shown are the analytical solutions of Petuhkov and Popov [Ref. 25], for turbulent heat transfer in round tubes given as:

$$Nu = \frac{(f/8) Re \ Pr}{k_1(f) + k_2(Pr)\sqrt{f/8} (Pr^{(2/3)} - 1)}$$

where 'f' the friction factor, has been calculated using the Filonenko equation given in Karlekar and Desmond [Ref. 40] as:

$$f = (1.82 \log Re - 1.64)^{-2}$$

and,

$$k_1(f) = 1 + 1.4f$$

$$k_2(Pr) = 11.7 + \frac{1.8}{Pr^{(1/3)}}$$

The analytical expression, given by Shibani and Ozisik [Ref. 26], for turbulent heat transfer between parallel plates:

$$Nu. = 12 + 0.03 Re^a Pr^b$$

where,

$$a = 0.88 - \frac{0.24}{(3.6 + Pr)}$$

$$b = 0.33 + 0.5 e^{-0.6 Pr}$$

valid for $0.1 < Pr < 10$, and $10^4 < Re < 10^6$, is also plotted.

While no conclusions can be drawn from the data obtained because it is not in the range of Reynolds numbers of these studies, it is worthy of note, that the present data as extrapolated, and the analytical and experimental works of others can be graphically shown to be close. It should also be noted that the investigations of Hsu [Ref. 34], Ashton [Ref. 33, and Haynes and Ashton [Ref. 32] all plotted experimental results between the Petukhov and Popov expression and that of Shibani and Ozisik, as shown graphically in the Haynes and Ashton study above.

The curved section data is plotted in Figure 13, and compared to the experimental work of Brinich and Graham [Ref. 31] for flow and mass transfer in a curved channel. The analytical solution of Petukhov and Popov, and Shibani and Ozisik are also plotted as a reference. A least squares correlation as given in Appendix C was used to extrapolate the data of Brinich and Graham. The accuracy of the data points used in this correlation are subject to errors, in that

the actual values were not given in their study and had to be taken from a plot of Stanton number versus Reynolds number as given in the reference.

Irrespective of the relatively small differences in the results and the correlations, the trends appear to be conclusive. The heat transfer rates can be seen to increase with increasing Reynolds number, and also that the heat transfer rate in a curved channel is measurably increased over that rate in a curved channel is measurably increased over that rate in a straight channel. This increase in heat transfer rate, appears to begin with the development of the Taylor-Goertler vortices and continues into the transition and turbulent flow regions. This result also appears to have been reached by K. V. Dement'eva and I. Z. Aronov [Ref. 41], who in 1978, investigating hydraulic resistance and heat transfer in curvilinear channels of rectangular cross-section, concluded that there was an enhancement of heat transfer intensity in curved rectangular corss-section channels as compared to straight pipes and channels.

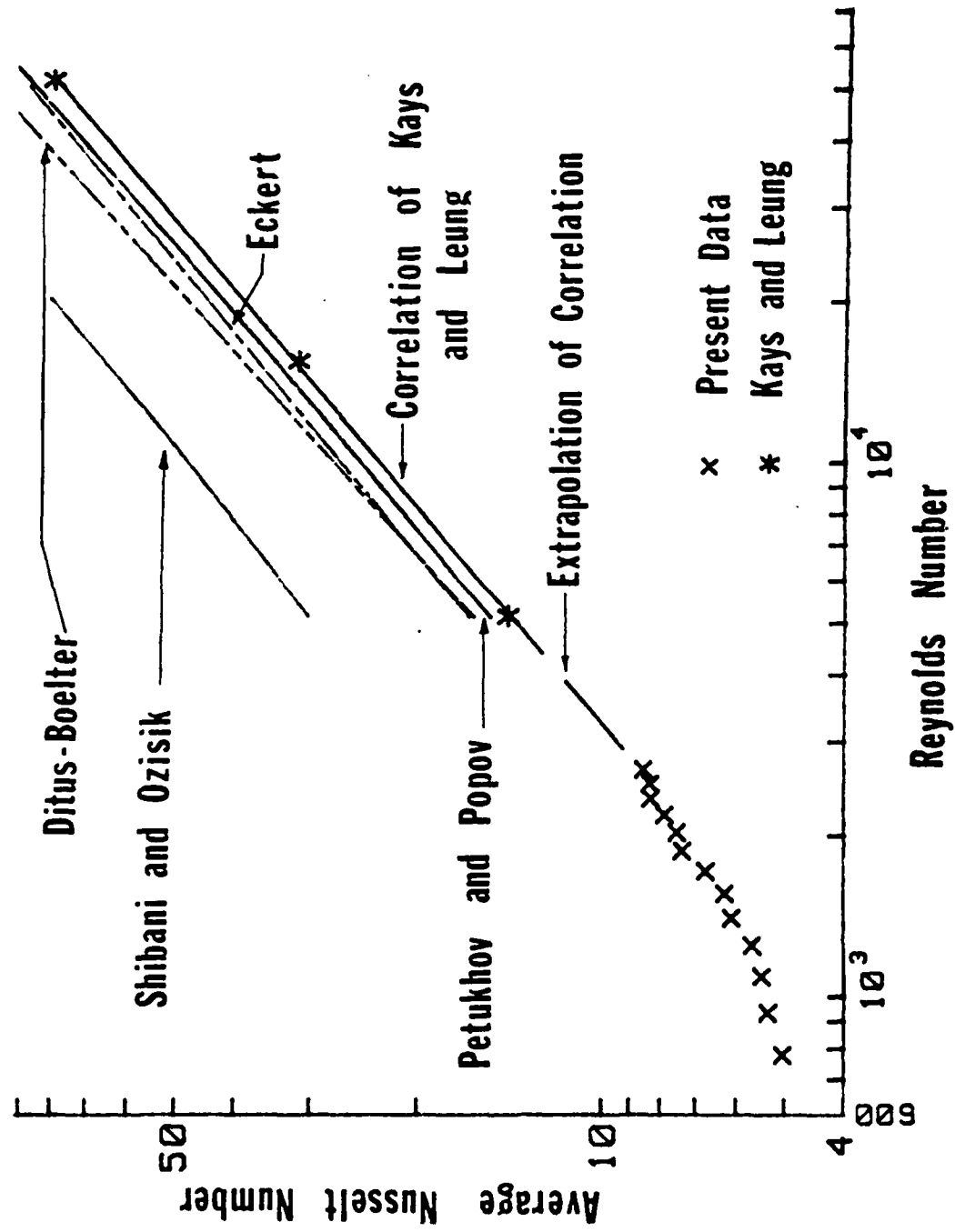


Figure 12. Comparison of present data for Transition Flows, Straight Section

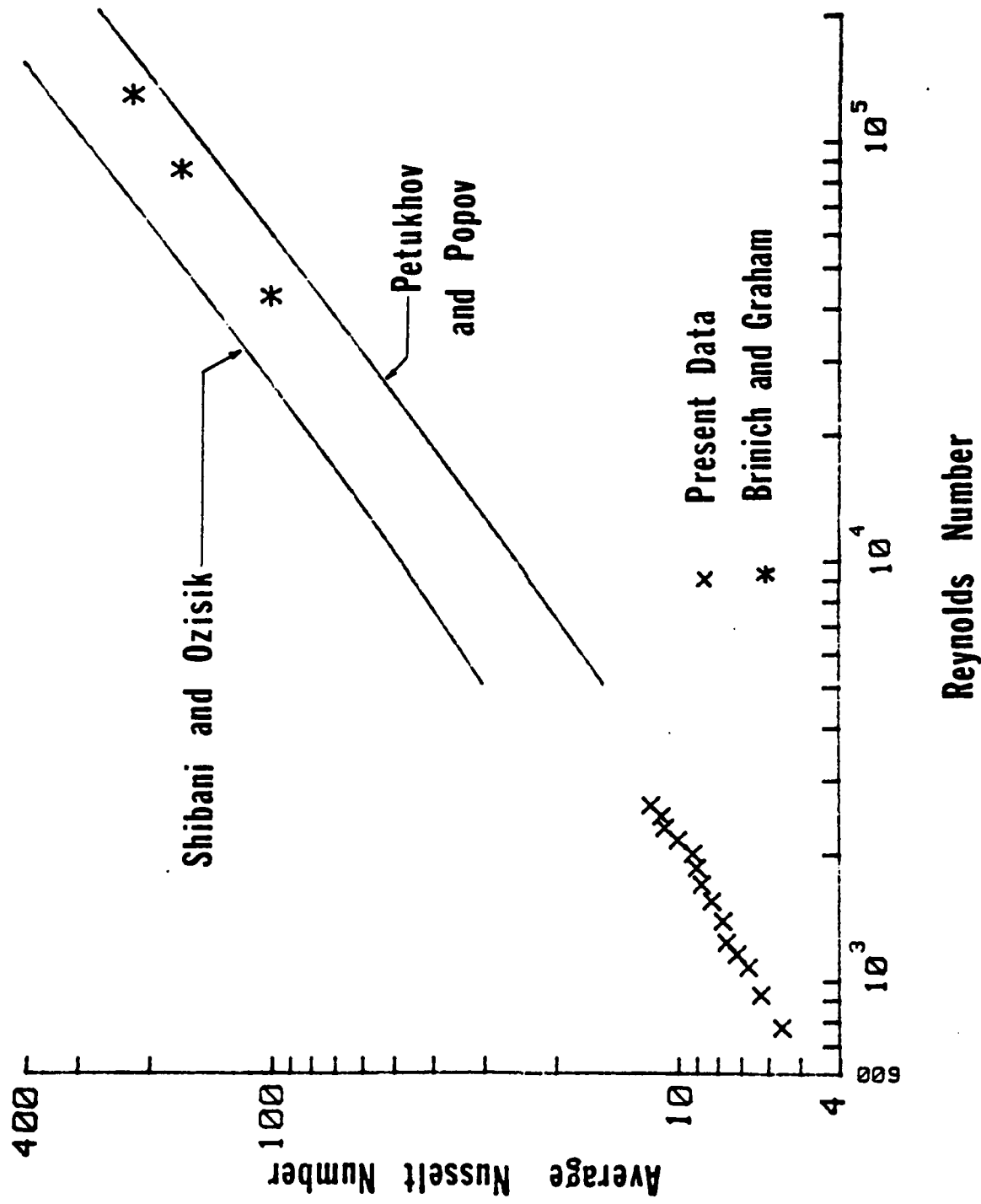


Figure 13. Comparison of Present Data for Transition Flows, Curved Section

VI. RECOMMENDATIONS

The amount of experimental work remaining in the study of heat transfer in curved channels is significant. Additional experiments in the transition region and in the fully turbulent region of fluid flow, should be conducted to refine the correlations for average Nusselt number. With this work, it would be necessary to design and construct a larger experimental configuration, capable of higher volumetric flow rate and greater temperature differences between the heated surface and the fluid inlet temperature. Additionally, care should be taken to ensure that the temperature of the exit flow, of each test section, is accurately measured. This may be accomplished by the use of a mixing cup arrangement at the exit flow locations. In a channel designed and constructed as the one in this study, care must be taken to allow for the removal of the mixing cup at the straight section exit location, to ensure that turbulence is not induced in the flow by the thermocouples prior to the fluid entering the curved section.

Also in the way of temperature measurement, a thermocouple should be installed at the entrance to the rotameter, or preferably some better device or means of determining the volumetric flow rate. This would ensure a more accurate measurement of the fluid temperature for an evaluation of the fluid properties in the mass flow calculation.

APPENDIX A: EXPERIMENTAL UNCERTAINTY

The uncertainties for the major variable in the experiments, were calculated in accordance by the method described by S. Kline and F. McClintoch [Ref. 42]. The estimates of the uncertainty in the measured quantities were made conservatively, and as such, there is considerable confidence in the uncertainties as calculated. An example of the calculations follows.

The Reynolds number was defined by the equation:

$$Re_d = \frac{\dot{m}d}{\mu_{air} A_c}$$

As such, the uncertainty was calculated by :

$$\frac{dRe_d}{Re_d} = \sqrt{\left(\frac{d\dot{m}}{\dot{m}}\right)^2 + \left(\frac{dd}{d}\right)^2 + \left(\frac{d\mu_{air}}{\mu_{air}}\right)^2 + \left(\frac{dA_c}{A_c}\right)^2}$$

The uncertainty in the mass flow rate was determined in a similar manner, by its equations:

$$\dot{m} = \frac{QP}{RT}$$

$$\text{and } \frac{d\dot{m}}{\dot{m}} = \sqrt{\left(\frac{dP}{P}\right)^2 + \left(\frac{dR}{R}\right)^2 + \left(\frac{dT}{T}\right)^2 + \left(\frac{dQ}{Q}\right)^2}$$

The uncertainties in the height of the channel, dynamics viscosity of air, cross-sectional area of the channel, the gas constant, pressure, temperature and the reading of the volumetric flow rate were obtained from estimates as:

$$\frac{dd}{d} = .01987, \frac{d\mu_{air}}{\mu_{air}} = .00223, \frac{dA_c}{A_c} = .01976$$

$$\frac{dR}{d} = .00002, \frac{dP}{P} = .00048, \frac{dT}{T} = .00055$$

$$\frac{dQ}{Q} = .0200$$

The uncertainty in the mass flow rate was then calculated as;

$$\frac{d\dot{m}}{\dot{m}} = .0200$$

and the Reynolds number uncertainty was

$$\frac{dRe_d}{Re_d} = \sqrt{(.0200)^2 + (.01987)^2 + (.00223)^2 + (.01976)^2} = .0345$$

$$Re_d = 2042 \pm 71$$

The uncertainty in the Nusselt number was also calculated in an identical manner, using the equation:

$$\overline{Nu} = \frac{\overline{h}d}{K_{air}}$$

and the uncertainty as

$$\frac{d\overline{Nu}}{\overline{Nu}} = \sqrt{\left(\frac{d\overline{h}}{\overline{h}}\right)^2 + \left(\frac{dd}{d}\right)^2 + \left(\frac{dK_{air}}{K_{air}}\right)^2}$$

It was therefore, necessary to first calculate the uncertainty for \overline{h} . Using the same approach,

$$\overline{h} = \frac{Q_{air}}{A_{PL}\Delta T}$$

and

$$\frac{d\overline{h}}{\overline{h}} = \sqrt{\left(\frac{dQ_{air}}{Q_{air}}\right)^2 + \left(\frac{dA_{PL}}{A_{PL}}\right)^2 + \left(\frac{d\Delta T}{\Delta T}\right)^2}$$

$$\text{where } \Delta T = T_{wo} - T_B$$

$$\frac{dA_{PL}}{A_{PL}} = .0026 \text{ and } \frac{d\Delta T}{\Delta T} = .0048$$

The uncertainty in Q_{air} was calculated by:

$$Q_{air} = \dot{m}C_{pair}(T_{OUT} - T_{IN})$$

and

$$\frac{dQ_{air}}{Q_{air}} = \sqrt{\left(\frac{d\dot{m}}{\dot{m}}\right)^2 + \left(\frac{dC_{Pair}}{C_{Pair}}\right)^2 + \left(\frac{d(T_{OUT} - T_{IN})}{T_{OUT} - T_{IN}}\right)^2}$$

where

$$\frac{d\dot{m}}{\dot{m}} = 0.0200, \frac{dC_{Pair}}{C_{Pair}} = .0042,$$

$$\text{and } \frac{d(T_{OUT} - T_{IN})}{T_{OUT} - T_{IN}} = .0623$$

These calculations result in the following uncertainties:

$$\frac{dQ_{air}}{Q_{air}} = .0656$$

$$\frac{dh}{h} = .0658$$

$$\frac{dNu}{Nu} = .0688$$

It is therefore, the uncertainty in the difference between outlet and inlet temperatures of the flowing air, that is ultimately the major source of average Nusselt number uncertainty. This then is the basis for the recommendation to better ascertain the exit temperatures for each test section. The calculations, as shown above, were for the 65% straight section run. Similar calculations for the curved section at 65% yield the following;

$$\frac{dRe_d}{Re_d} = .0345$$

$$Re_d = 2038 \pm 70$$

$$\frac{dNu}{Nu} = .0563$$

$$\bar{Nu} = 9.34 \pm 0.525.$$

The values for the uncertainties for all the variables in the curved section test run are as follows:

<u>QUANTITY</u>	<u>UNCERTAINTY</u>
A_{PL}	.0026
A_c	.0198
C_p	.0042
d	.0199
D_e	.0398
h	.0526
K_{air}	.0003
\bar{Nu}	.0563
\dot{m}	.0200
Q	.0200
Q_{air}	.0523
Re	.0345
T_B	.0073
T_{IN}	.0029
T_{OUT}	.0106
T_w	.0060
$T_{OUT} - T_{IN}$.0482
ΔT	.0047
μ	.0022
ρ	.0007

APPENDIX B: SAMPLE CALCULATIONS

A sketch of the control volume for the energy balance, for the straight section, indicating the major heat transfer components is shown in Figure 14. The sample calculations that follow, show the methods and equations that were used to obtain these heat transfer components. The heat transfer components were required to satisfy the energy balance, and to obtain an average Nusselt number as a function Reynolds number of the flowing air.

The curved section energy balance and calculations are similar

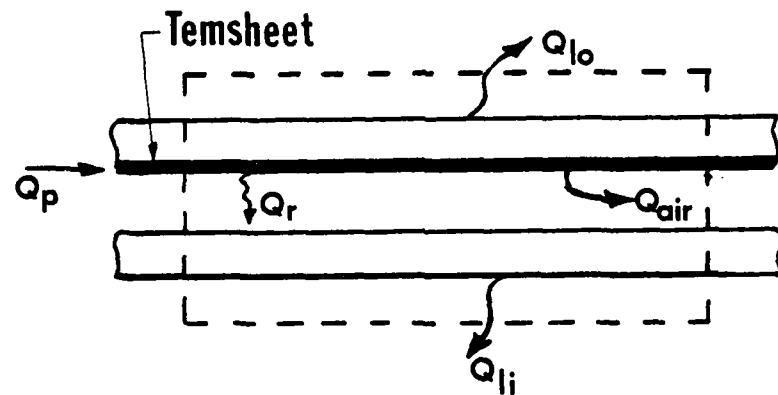


FIGURE 14. Energy balance in straight section

A. SAMPLE CALCULATIONS DATA

T_{ROOM}	= 21.6°C
Q	= 55%
V_{PR}	= 3.2165 V
V_H	= 37.1210 V
R_{PR}	= 2.078
T_{IN}	= 0.839 mV = 21.82°C
T_{INS1}	= 1.324 mV = 33.34°C
T_{INS2}	= 1.583 mV = 39.45°C
$Two1$	= 1.840 mV
$Two2$	= 1.840 mV
$Two3$	= 1.987 mV
$Two4$	= 2.001 mV
$Two5$	= 2.112 mV
$Two6$	= 2.125 mV
$Two7$	= 2.245 mV
$Two8$	= 2.241 mV
$Tw11$	= 0.964 mV
$Tw12$	= 0.967 mV
$Tw13$	= 1.012 mV
$Tw14$	= 1.008 mV
$Tw15$	= 1.056 mV
$Tw16$	= 1.047 mV
$Tw17$	= 1.101 mV
$Tw18$	= 1.100 mV
T_{OUT}	= 1.124 mV = 27.97°C
T_{EXIT}	= 1.076 mV = 26.91°C = 80.44°F
A_{PL}	= 0.0742 m ²

$$\begin{aligned}
A_c &= 0.0016 \text{ m}^2 \\
d &= 0.00635 \text{ m} \\
K_{air} &= 0.02662 \text{ W/m}^\circ\text{C} \\
C_{Pair} &= 1.0057 \text{ KJ/Kg}^\circ\text{C} \\
\mu_{air} &= 1.983 \times 10^{-5} \text{ Kg/m.sec} \\
K_{INS} &= 4.18 \times 10^{-2} \text{ W/m}^\circ\text{C} \\
\Delta x_{INS} &= 0.00635 \text{ m} \\
\epsilon_{wo} &= 0.70 \\
\epsilon_{wi} &= 0.40 \\
F_{wo-wi} &= 1.0 \\
\sigma &= 5.669 \times 10^{-8} \text{ W/m}^2 \text{ }^\circ\text{K}
\end{aligned}$$

B. TEMPERATURE CALCULATIONS

1. Temperature Difference in Insulation (ΔT_{INS})

$$\Delta T_{INS} = T_{INS2} - T_{INS1} = 39.45 - 33.34 = 6.11^\circ\text{C}$$

2. Bulk Temperature (T_B)

$$T_B = \frac{T_{IN} + T_{OUT}}{2} = \frac{21.82 + 27.97}{2} = 24.90^\circ\text{C}$$

3. Mean Temperature Difference (ΔT)

$$\Delta T = T_{wo} - T_B = 50.09 - 24.90 = 25.19^\circ\text{C}$$

C. POWER CALCULATIONS

1. Power Supplied (Q_p)

$$Q_p = \frac{V_{PR} V_H}{R_{PR}} = \frac{(3.2165)(37.121)}{(2.078)} = 57.46 \text{ W}$$

2. Heat Lost Through Outer Plate (Q_{Lo})

$$\begin{aligned}
Q_{Lo} &= \frac{\Delta T_{INS}}{\Delta x_{INS}/K_{INS} \cdot A_{PL}} = \frac{6.11}{(0.00635)/((4.18 \times 10^{-2})(0.0742))} \\
&= 2.98 \text{ W}
\end{aligned}$$

3. Heat Radiated (Q_r)

a. Radiation Resistance (R_R)

$$R_R = \frac{1 - \epsilon_{wo}}{A_{PL} \epsilon_{wo}} + \frac{1}{A_{PL} F_{wo-wi}} + \frac{1 - \epsilon_{wi}}{A_{PL} \epsilon_{wi}}$$

$$= \frac{1}{A_{PL}} \left[\frac{1}{\epsilon_{wo}} + \frac{1}{\epsilon_{wi}} - 1 \right] = \frac{2.929}{A_{PL}}$$

b. Heat Radiated (Q_r)

$$Q_r = \frac{\sigma (T_{wo}^4 - T_{wi}^4)}{R_R} \quad T = {}^\circ K$$

$$= \frac{(5.669 \times 10^{-8})(0.0742)(323.25^4 - 298.92^4)}{2.929}$$

$$= 4.214 \text{ W}$$

4. Heat Convected to Air (Q_{air})

a. Corrected Volumetric Flow Rate (\dot{q})

$$\dot{q} = Q \sqrt{\theta} = Q \frac{T_{EXIT}({}^\circ R)}{T_{STANDARD}({}^\circ R)}$$

$$= \frac{(0.793)(0.55)}{60} \quad \frac{540.13}{529.69}$$

$$= 0.0073 \text{ m}^3/\text{sec}$$

b. Density (ρ)

$$\rho = \frac{P}{R T_{EXIT}} = \frac{101325}{(297)(26.91 + 273.16)}$$

$$= 1.177 \text{ Kg/m}^3/\text{sec}$$

c. Mass Flow Rate (\dot{m})

$$\dot{m} = \dot{q}_p = (0.0073)(1.177) = 0.0086 \text{Kg/sec}$$

d. Heat Convected to Air (Q_{air})

$$\begin{aligned} Q_{air} &= \dot{m} C_{Pair} (T_{OUT} - T_{IN}) \\ &= (0.0086)(1.0057)(27.97 - 21.82) \\ &= 0.05319 \text{ KJ/sec} \\ &= 53.19 \text{ W} \end{aligned}$$

D. AVERAGE HEAT TRANSFER COEFFICIENT (\bar{h})

$$\begin{aligned} \bar{h} &= \frac{Q_{air}}{A_{PL} \Delta T} = \frac{53.19}{(0.0742)(25.19)} \\ &= 28.46 \text{ W/M}^2 \text{ }^\circ\text{C} \end{aligned}$$

E. AVERAGE NUSSELT NUMBER (\bar{Nu})

$$\bar{Nu} = \frac{\bar{h}d}{K_{air}} = \frac{(28.46)(0.00635)}{(0.02662)} = 6.789$$

F. REYNOLDS NUMBER (Re)

$$\begin{aligned} Re_d &= \frac{\dot{m} d}{\mu_{air} A_c} = \frac{(0.0086)(0.00635)}{(1.983 \times 10^{-5})(0.0016)} \\ &= 1721.19 \\ &= 1721 \end{aligned}$$

APPENDIX C: CORRELATIONS

All correlations were obtained using the method of least squares (first degree polynomial), as outlined by C. F. Gerald [Ref. 43]. In this method the values of Reynolds number (x) and Nusselt number (Y) were first converted to the appropriate natural logarithmic value, after which the summations of x_i , x_i^2 , Y_i , and $x_i Y_i$ were calculated. The values of these quantities were then placed in a matrix to solve the simultaneous equations:

$$a_0 N + a_1 \sum x_i = \sum Y_i$$

$$a_0 \sum x_i + a_1 \sum x_i^2 = \sum x_i Y_i$$

where N is the number of data points, and the matrix is

$$\begin{bmatrix} N & \sum x_i \\ \sum x_i & \sum x_i^2 \end{bmatrix} \begin{bmatrix} a_0 \\ a_1 \end{bmatrix} = \begin{bmatrix} \sum Y_i \\ \sum x_i Y_i \end{bmatrix}$$

After attaining the values of a_0 and a_1 , the equation of the line became:

$$\ln \bar{Nu} = a_0 + a_1 \ln Re$$

or

$$\bar{Nu} = e^{a_0} Re^{a_1}$$

The quantities for the various studies are given in Table III.

The standard deviation for the present study curved section correlation was calculated as:

$$\sigma^2 = \frac{\sum (Y_i - y_i)}{N-n-1}$$

where: Y_i is the actual value of average Nusselt number obtained in the test runs

y_i is the value of average Nusselt number calculated from the correlation equation

N is the number of data points used in the correlation

n is the degree polynomial used.

The result of the above method was

$$\sigma^2 = .02426$$

TABLE III: CORRELATIONS

STUDY	SECTION	NUMBER OF POINTS	Σx_i	Σx_i^2	Σy_i	$\Sigma x_i y_i$	FLOW
DURAO	STRAIGHT	3	19.98	133.2	4.70	31.34	LAMINAR
BALLARD	STRAIGHT	5	33.55	255.1	8.23	55.25	LAMINAR
PRESENT STUDY	STRAIGHT	2	13.51	91.3	3.31	22.35	LAMINAR
KAYS & LEUNG	STRAIGHT	3	29.03	283.6	10.48	103.4	TURBULENT
PRESENT STUDY	STRAIGHT	9	66.84	496.9	17.29	128.7	TRANSITION
BRINICH & GRAHAM	CURVED	3	33.81	381.6	15.1	170.6	TURBULENT
PRESENT STUDY	CURVED	9	66.11	486.1	19.15	140.9	TRANSITION

LIST OF REFERENCES

1. Taylor, G. I., "Stability of a Viscous Liquid Contained Between Two Rotating Cylinders", Philosophical Transactions of the Royal Society of London, series A, V.233, pp. 289-343, 1923.
2. National Advisory Committee for Aeronautics, Technical Memorandum 1375, On the Three Dimensional Instability of Laminar Boundary Layers on Concave Walls, by H. Gortler, 1942.
3. Smith, A.M.O., "On the Growth of Taylor-Gortler Vortices Along Highly Concave Walls", Quarterly of Applied Mathematics, V. 8, pp. 233-262, November 1955.
4. Kreith, F., "The Influence of Curvature on Heat Transfer to Incompressible Fluids", Trans. ASME, V. 77, pp. 1247-1256, 1955.
5. Mori, Y., and Uchida, Y., "Forced Convective Heat Transfer Between Horizontal Flat Plates", International Journal of Heat and Mass Transfer, V.9, pp. 803-817, 1966.
6. Tobak, M., "Hypothesis for the Origin of Cross-Hatching", AIAA Journal, V.8, No. 2, pp. 330-334, February 1970.
7. Mayle, R.E., Kopper, F.C., Blair, M.F., and Bailey, D.A., "Effect of Streamline Curvature on Film Cooling", Journal of Engineering for Power, Trans. ASME, V.99, Series A, No. 1, pp. 77-82, January 1977.
8. Nicolas, J. and LeMeur, A., "Curvature Effects on a Turbine Blade Cooling Film", ASME Paper No. 74-GT-156.
9. Folayan, C.O. and Whitelaw, J. H., "The Effectiveness of Two-Dimensional Film-Cooling Over Curved Surfaces", ASME Paper No. 76-HT-31.
10. Lord Raleigh, "On the Dynamics of Revolving Fluids", Proceedings of the Royal Society of London, series A, V.93, pp. 148-154, 1916. Reprints in Scientific Papers, V.6, pp. 447-453.

11. Taylor, G.I., "Distribution of Velocity and Temperature Between Concentric Rotating Cylinders", Proceedings of the Royal Society of London, series A, V.151, pp. 494-512, 1935.
12. Dean, W.R., "Fluid Motion in a Curved Channel", Proceedings of the Royal Society of London, series A, V.121, pp. 402-420, 1928.
13. Reid, W.H., "On the Stability of Viscous Flow in a Curved Channel", Proceedings of the Royal Society of London, series A, V.244, pp. 186-198, 1958.
14. Schlichting, H., Boundary Layer Theory, 7th ed., pp. 529-536, McGraw-Hill, 1979.
15. Kelleher, M.D., Flentie, D.L., and KcKee, R.J., "An Experimental Study of the Secondary Flow in a Curved Rectangular Channel", Journal of Fluids Engineering, V.102, pp. 92-96, March 1980.
16. Winoto, S.H., Durao, D.F.G., and Crane, R.I., "Measurement within Gortler Vortices", Journal of Fluids Engineering, V.101, pp. 517-520, December 1979.
17. Aihara, Y., "Nonlinear Analysis of Gortler Vortices", The Physics of Fluids, V.19, pp. 1655-1660, November 1976.
18. Aerospace Research Laboratories Report ARL 65-68, A Simplified Approach to the Influence of Gortler-Type Vortices on the Heat-Transfer from a Wall, by Leif N. Persen, May 1965.
19. McCormack, P.D., Welker, H., and Kelleher, M.D., "Taylor-Gortler Vortices and Their Effect on Heat Transfer", Journal of Heat Transfer, V.92, pp. 101-112, February 1970.
20. Kahawita, R. and Meroney, R., "The Influence of Heating on the Stability of Laminar Boundary Layers Along Concave Curved Walls", Journal of Applied Mechanics, V.99, pp. 11-17, March 1977.
21. Akiyama, M., Hwang, G.J., and Cheng, K.C., "Experiments on the Onset of Longitudinal Vortices in Laminar Forced Convection Between Horizontal Plates", Journal of Heat Transfer, V.93, pp. 335-341, November 1971.

22. Cheng, K.C., and Akiyama, M., "Laminar Forced Convection Heat Transfer in Curved Rectangular Channels", International Journal of Heat and Mass Transfer, V.13, pp. 471-490, 1970.
23. Yee, G, and Humphrey, J.A.C., "Developing Laminar Flow and Heat Transfer in Strongly Curved Ducts of Rectangular Cross Section", ASME Paper No. 79-WA/HT-15.
24. Cheng, K.C., Lin, R.C., and Ou, J.W., "Graetz Problems in Curved Square Channels, ASME Paper No. 75-HT-EE, San Francisco, California, 11 August 1975.
25. Petukhov, B.S. and Popov, V.N., "Theoretical Calculation of Heat Exchange and Frictional Resistance in Turbulent Flow in Tubes of an Incompressible Fluid with Variable Physical Properties, Trans. in High Temperatures, V.1, No. 1, pp. 69-83, 1963.
26. Shibani, A.A., and Ozisik, M.N., A Solution to Heat Transfer in Turbulent Flow Between Parallel Plates. International Journal of Heat and Mass Transfer, V.20, pp. 65-573, 1977.
27. Mori, Y., Uchida, Y, and Ukon, T., "Forced Convective Heat Transfer in a Curved Channel with a Square Cross Section", International Journal of Heat and Mass Transfer, V.14, pp. 1787-1805, 1971.
28. Kays, W.M. and Leung, E.Y., Heat Transfer in Annular Passages - Hydrodynamically Developed Turbulent Flow with Arbitrarily Prescribed Heat Flux, International Journal of Heat and Mass Transfer, V.6, pp. 507-557, 1963.
29. Durao, M. do Carmo, Investigation of Heat Transfer in Straight and Curved Rectangular Ducts Using Liquid Crystal Thermography, Eng. Thesis, Naval Postgraduate School, Monterey, California, 1977.
30. Ballard, J.C. III, Investigation of Heat Transfer in Straight and Curved Rectangular Ducts., Masters Thesis, Naval Postgraduate School, Monterey, California, 1980.
31. Brinich, P.F. and Graham, R.W., Flow and Heat Transfer in a Curved Channel, NASA Technical Note No. TN-D-8464, 1977.

32. Haynes, F.D. and Ashton, G.D., "Turbulent Heat Transfer in Large Aspect Ratio Channels", Journal of Heat Transfer, V.102, No. 2, pp. 384-386
33. Ashton, G. D., The Formation of Ice Ripples on the Under-side of River Ice Covers, Thesis, presented in partial fulfillment of requirements for degree of Doctor of Philosophy, University of Iowa, 1971.
34. Hsu, K., Spectral Evolution of Ice Ripples, Thesis presented in partial fulfillment of requirements for degree of Doctor of Philosophy, University of Iowa, 1973.
35. Department of Mechanical Engineering, -Stanford University, Report No. AHT-3, Heat Transfer with Laminar and Turbulent Flow Between Parallel Planes with Constant and Variable Wall Temperature and Heat Flux, by P.A. McCuen, W. M. Kays, and W.C. Reynolds, 12 April 1962.
36. Worse-Schmidt, P.M., "Heat Transfer in the Thermal Entrance Region of Circular Tubes and Annular Passages with Fully Developed Laminar Flow", International Journal of Heat and Mass Transfer, V.10, pp. 541-551, 1967.
37. Shah, R.K. and London, A.L., Laminar Flow Forced Convection in Ducts, Supplement 1, pp. 305-312, Academic Press, 1978.
38. Gebhart, B. Heat Transfer, 2nd ed, p. 260, McGraw-Hill, New York, 1971.
39. Eckert, E.R.G., Introduction to Heat and Mass Transfer, p. 112, McGraw-Hill, 1950.
40. Karlekar, B.V. and Desmond, R.M., Engineering Heat Transfer, p. 560, West Publishing Company, 1977.
41. Dement'eva, K.V. and Aronov, I.Z., Hydrodynamics and Heat Transfer in Curvilinear Channels of Rectangular Cross Section. Journal of Engineering Physics, V.34, No. 6, pp. 666-671, 1978.
42. Kline, S.J. and McClintock, F.A., "Describing Uncertainties in Single-Sample Experiments", Mechanical Engineering, V.75, pp. 3-8, January 1953.
43. Gerald, C.F., Applied Numerical Analysis, 2nd ed. pp. 465-74, Addison-Wiley Publishing Company, 1978.

INITIAL DISTRIBUTION LIST

	No. Copies
1. Defense Technical Information Center Cameron Station Alexandria, Virginia 22314	2
2. Library, Code 0142 Naval Postgraduate School Monterey, California 93940	2
3. Department Chairman, Code 69 Department of Mechanical Engineering Naval Postgraduate School Monterey, California 93940	1
4. Associate Professor M. D. Kelleher, Code 69Kk Department of Mechanical Engineering Naval Postgraduate School Monterey, California 93940	2
5. LCDR R. G. Holihan, Jr., USN Supervisor of Shipbuilding Conversion and Repair, USN Gen. Dyn. Corp. Electric Boat Div. Groton, Connecticut 06340	2

DAU
ILM